Understanding Air Quality Trends in Europe

Focus on the relative contribution of changes in emission of activity sectors, natural fraction and meteorological variability

May 2021

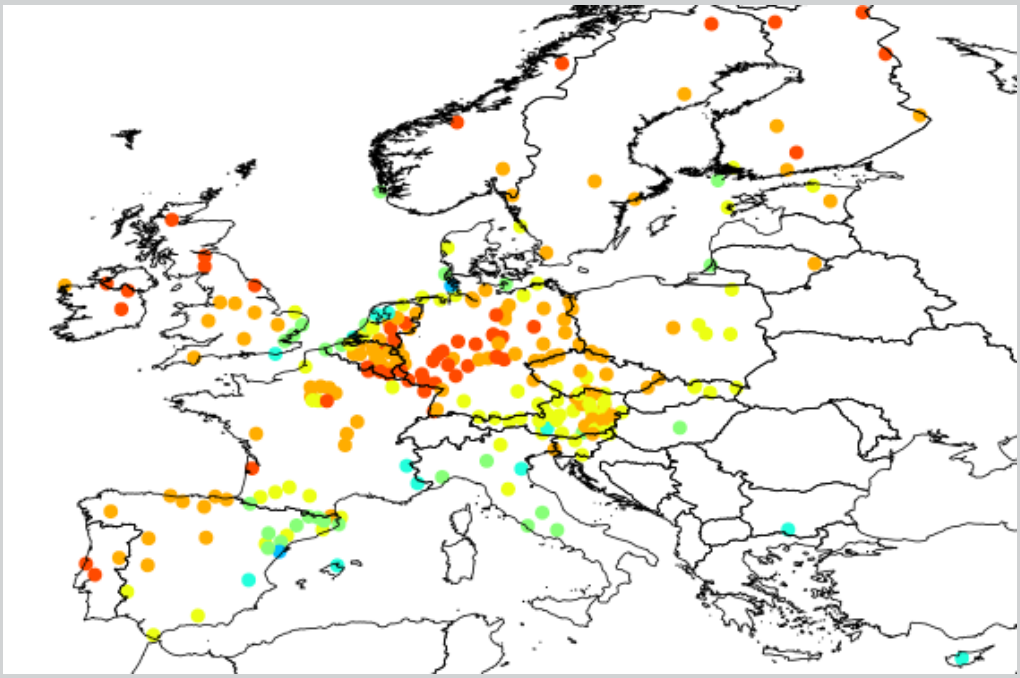

Authors:
Colette, A. (INERIS), Solberg, S. (NILU), Aas, W. (NILU), Walker, S.-E. (NILU)

ETC/ATNI consortium partners:
NILU – Norwegian Institute for Air Research, Aether Limited, Czech Hydrometeorological Institute (CHMI), EMISIA SA, Institut National de l'Environnement Industriel et des risques (INERIS), Universitat Autònoma de Barcelona (UAB), Umweltbundesamt GmbH (UBA-V), 4sfera Innova, Transport & Mobility Leuven NV (TML)

European Environment Agency
European Topic Centre on Air pollution, transport, noise and industrial pollution

Cover design: ETC/ATNI
Cover photo © ETC/ATNI
Layout: ETC/ATNI

The withdrawal of the United Kingdom from the European Union did not affect the production of the report.
Data reported by the United Kingdom are included in all analyses and assessments contained herein, unless otherwise indicated.

Author(s)
Aμgustin Colette (INERIS), Sverre Solberg (NILU), Wenche Aas (NILU), Sam-Erik Walker (NILU)

ETC/ATNI c/o NILU
ISBN 978-82-93752-25-7

European Topic Centre on Air pollution,
transport, noise and industrial pollution
c/o NILU – Norwegian Institute for Air Research
P.O. Box 100, NO-2027 Kjeller, Norway
Tel.: +47 63 89 80 00
Email: etc.atni@nilu.no
Web : https://www.eionet.europa.eu/etcs/etc-atni

Contents

Summary 4

1 Introduction 7

2 Methods 8

2.1 GAM model 8

2.2 EMEP/MSC-W 8

2.3 Observations 9

2.4 Trend calculations 9

3 Validation 10

3.1 Ozone 10

3.2 NO_2 13

3.3 PM_{10} 16

4 Results 19

4.1 Meteorological decomposition 19

4.1.1 Time series 2000-2017 19

4.1.2 Interannual variability due to meteorology and other factors. 22

4.2 Precursor trends 28

4.3 Trends in atmospheric composition 30

4.4 Trends in PM_{10} and $PM_{2.5}$ and source contributions 33

5 References 38

Summary

We present an analysis of air quality trends in Europe aiming to identify the relative contribution of the main factors influencing ambient air quality. The main pollutants under focus are ozone, nitrogen dioxide and particulate matter for which a dense enough network of observation is available to derive robust conclusion on the overall air quality in Europe. Air pollutant concentrations are primarily driven by the European emission of anthropogenic precursors, meteorological variability driving the accumulation and transformation of pollutants, and long-range transport at hemispheric scale.

Substantial improvements are observed in ambient air over the period 2000-2017 according to AQ e-reporting monitoring stations. PM_{10} particulate matter decreases by 25 to 45%. For ozone peaks (as the fourth highest daily maximum of 8-hr mean: 4MDA8) the decrease is only about 10%, whereas the improvement in one of the main precursors, the ambient NO_2, is 30%. The reported anthropogenic emissions of NOx reduction in Europe reach 53% over the same period (Colette and Rouïl, 2020).

The mismatch between those estimates raise legitimate question on a possible discrepancy between reported emission trends and actual efficiency of mitigation measures (in particular for NOx), but also on the possible role of external factors such as meteorological variability, natural emissions, or hemispheric transport for ozone and particulate matter.

To address this question, we rely on two complementary modelling approaches, (i) chemistry-transport modelling (CTM) and (ii) machine learning statistical models. The CTM employed here is the EMEP MSC-W model used in policy support activities in the framework of the United Nations Convention on Long-range transboundary air pollution (CLRTAP). The machine learning model is a Generalized Additive Model (GAM) developed by ETC/ATNI to reproduce the meteorological sensitivity of European air pollution.

Both models are confronted against in-situ monitoring stations from the Airbase and AQ e-reporting databases (therefore also including most EMEP sites). Only stations with data coverage at least 75% of the years over the 2000-2017 period were included. This drastically reduces the number of monitoring sites and the spatial representativity of the assessment, and is biased towards countries benefiting from a long-term monitoring network.

For ozone, the GAM and CTM model display similar performances in capturing the interannual variability of high ozone peaks, but the GAM is notably better for the intra-annual variability of daily maxima. Both perform better over Western, Central and Northern Europe than over Mediterranean areas. For NO_2, the GAM model captures much better the interannual variability throughout Europe. For PM_{10}, the performances of the GAM and CTM are closer, with yet a slight advantage to the GAM compared to the CTM.

The two models can be used to assess the relative importance of driving factors on ambient air. In the sensitivity simulations investigated here, the GAM model isolates the contribution of (i) meteorological variability and (ii) emissions and background. The CTM scenarios investigated here isolate the contributions of (i) meteorological variability and background and (ii) emissions. This difference in design unfortunately precludes a clear comparison between both approaches. There are however some clear conclusions that can be drawn from this comparison:

- Emission changes are the main driver to all air pollutant trends. For NO_2 and PM_{10}, it is clear from both GAM and CTM results that this driver dominates and contributes to at least 90% of the 2000-2017 trend.
- For ozone peaks (as 4MDA8), the meteorological factor can be important for the 2000-2017 trend. The GAM model estimates that it contributes to an increase counteracting mitigation effort up to a magnitude of 20 to 80% (compared to the effect of emission and background changes) in Austria, Belgium, Czech Republic, France and Italy. Given the good skill of the GAM model to capture meteorological effect, this estimate can be considered quite robust.

The CTM sensitivity simulations investigated here include both meteorology and background changes. They confirm that such factors can be important for the trends, also reaching 20-150% (compared to the effect of emission changes) depending on the countries, but generally contributing to decreasing trends (therefore acting in the same direction as European mitigation strategies). This decrease is largely influenced by ozone boundary conditions that follow a decreasing trend in the model simulations. From the simulations analysed here it is not possible to conclude whether the CTM would have indicated a similar meteorological penalty as the GAM that would have been compensated by hemispheric contribution.

These results demonstrate the substantial impact of factors such as meteorological variability or background changes for ozone peaks, whereas European emission changes dominate for PM_{10} and NO_2 trends.

We then extend the analysis to natural factors and individual activity sectors. Such an analysis can only be performed for PM and precursors, and on the basis of the EMEP monitoring sites or CTM results as the GAM model is only designed to capture meteorological factors.

The joint analysis of EMEP model and measurements results show a significant reduction in both PM_{10} and $PM_{2.5}$ (0.28 µg mg^{-3} y^{-1} and -1.7-2.0 % y^{-1}). The decrease in sulphate explains 22-29% of the reductions in PM_{10} while nitrate and ammonium explain each around 10% of the PM_{10} trend in the observations. The model estimates a higher role of nitrate and ammonium to the PM_{10} trend (25% and 14% respectively). Observed trends in organic aerosols indicate that this may be important, but too few data and large uncertainties in the trend precludes validation against the model estimates.

The EMEP CTM can be used to infer how the contribution from different sectors have changed over time.

The relative contribution of agriculture and industry to the total PM_{10} mass has been reduced by around 30% for both sectors. This similar evolution is not directly linked to the emission trends in the respective sectors, it is a nonlinear relationship depending on availability of precursor gases to form ammonium sulphate and ammonium nitrate. The relative contribution of traffic sources to PM_{10} has been reduced with around 20%, while the trend attributed to residential heating is marginal. The model also indicates that the natural contributions (such as sea salt and dust) has had little impact on the long-term changes in PM_{10}.

These results demonstrate that measures to reduce emissions of precursor gases from several sectors explain the PM reductions in Europe. The heating sector has become a relatively more important contributor to the aerosol pollution and needs more attention. In addition, further methods development to reduce the uncertainties in both modelling and observations of organic aerosols from the residential heating sector is needed.

Acknowledgements

This report is a part of ETC/ATNI AP2020 deliverables. The EEA task manager was Evrim Ozturk.

Αμgustin Mortier from EMEP MSC-W and MET Norway is greatly acknowledged for all help in facilitating data from the EMEP web trend interface (https://aerocom-trends.met.no/EMEP/). Hilde Fagerli and Svetlana Tsyro also from EMEP MSC-W have been very helpful in the discussion of the EMEP results.

1 Introduction

Context:

- The present report aims to strengthen our understanding of air quality trends in Europe on the basis of the analysis of in-situ observation available in the AQ e-reporting database, supplemented by additional information from air quality models. We take stock of past assessment performed by ETC/ACM and ETC/ATNI and focus essentially on providing more insight on how meteorological variability, natural factors, and emission from the main activity sectors might have influence the trend in PM_{10}, NO_2 and Ozone between 2000 and 2017.

Motivation:

- Documenting the long term evolution of air quality trends in Europe is an important topic, in particular to understand to what extent an improvement is found in terms of detrimental impacts on human health (Colette et al., 2017a) or ecosystems (Colette et al., 2018).

Availability of air quality observations:

- A few years ago, such long term trend analyses could only be performed on the basis of a limited set of reference sites such as the EMEP network (Colette et al., 2016).
- The first studies including a wider range of regulatory air quality monitoring stations (including urban sites) were limited in terms of spatial coverage with long terms records available only for a few countries in Western Europe (Colette et al., 2015).
- Long term air quality observations are now available over a much larger dataset of sites, the most recent assessment (Colette et al., 2019) relied on about 3,500 stations passing the requirement in terms of completeness of observations over the 2000-2017 period.

Such assessment on how air quality trends evolve also raise legitimate questions on the main drivers influencing the trend:

- Atmospheric composition is notoriously complex because of the non-linear chemical reaction involved, which are also influenced by (i) the local emission of anthropogenic of air pollutants, (ii) long range transport, (iii) biogenic and natural sources, (iv) meteorological variability. Quantifying the respective importance of each of these factors is then crucial to conclude on the efficiency of mitigation measures.
- Chemistry-Transport models can be used for such a quantitative decomposition of each of those factors as documented in the ETC/ACM Technical Report 2016/7 building upon the Eurodelta-Trends experiment coordinated under EMEP (Colette et al., 2017b).
- Statistical models can also be developed to isolate the impact of the meteorological factor. The first development in that direction were explored for ozone (Solberg. et al., 2015;Solberg et al., 2018b). It was extended to NO_2 and PM (Solberg et al., 2018a), and a synthesis was presented in (Solberg et al., 2020a).

In the present report:

- We put in perspective statistical versus chemistry-transport models to quantify the impact of meteorology on air quality trends
- We also discuss the impact of activity sectors and natural factors, which can only be done on the basis of chemistry transport models.

For this work we rely on:

- Statistical models developed internally by ETC/ATNI
- Chemistry-Transport model results made available to ETC/ATNI by EMEP/MSC-W.

2 Methods

2.1 GAM model

A Generalized Additive Model (GAM) is a non-linear regression model linking expected values of a given response variable to several explanatory variables. A GAM could be considered an extension of a standard MLR (multiple regression model) in which the coefficients are replaced by smooth functions. The GAM used in this study has been developed for several years for the assessment of air pollutant trends in Europe based on long-term monitoring data of O_3, NO_2, and PM. The aim has been to apply and adapt for European conditions a statistical method that has been used by the US-EPA on a routine basis for surface ozone trend assessments, adjusting for the inter-annual impact of changing meteorology.

The response variable in the GAM is a measured air pollutant (O_3, NO_2, PM_{10}) while the explanatory variables are represented by local, gridded meteorological data (temperature, relative humidity etc) as well as temporal variables (day of week, season and time since the start of the data series). The GAM is applied to time series of daily data for air pollutant concentrations and meteorology, and in the present study, we used data for the period 2000-2017.

The GAM was based on monitoring data from EEA (AirBase and e-reporting) available by download from EEA's web page as well as on meteorological data extracted from ECMWF (ERA-Interim as described by Dee et al., 2011).

All available EEA monitoring sites fulfilling a data capture criterion that 75 % of the data should exist in at least 75 % of the years in this period were used. The GAM was then applied to each monitoring station and parameter (NO_2, O_3, PM) individually. The main outcome of the GAM is that it optimises the fit to the observations and furthermore, that it estimates an individual response function between each explanatory variable and the response function. Thus, the influence of the long-term trend is separated from the changing influence of the meteorology. Any trends caused by meteorology alone could therefore also be calculated. The GAM and its applications is further described in (Solberg et al., 2020a;Solberg. et al., 2015;Solberg et al., 2020b).

2.2 EMEP/MSC-W

EMEP/MSC-W produces annually air quality simulations in support of the LRTAP Convention. This work is often complemented with long-term simulation to assess long term evolution. In 2019, it was even complemented by a sensitivity simulation covering the 2000-2017 period, but with anthropogenic emissions fixed at their levels for 2017. The comparison of this simulation with the reference trend simulation allows isolating the relative impact on the trends of (i) European anthropogenic emission changes and (ii) all the other factors (meteorological variability, natural sources, intercontinental transport).

The reference run is denoted EMEP_MSCW in the figures, and the simulation with constant emissions is EMEP_MSCW_2017. The trend of all factors besides emission changes is derived from the trend in EMEP_MSCW_2017, and simply subtracted from the trend in EMEP_MSCW to have the trend due to emissions alone.

In the trends comparing with EMEP observations, and for calculating changes in source contribution from different activities and in chemical composition, the consistent EMEP MSC-W model version available from the Aerocom trend tool is used (https://aerocom-trends.met.no/EMEP/) i.e.: Model versions rv4.17a and rv4.33 (for 2017) and Emissions EMEP v2018 and v2019 (for 2017). The impacts of different emission sectors on PM_{10} and $PM_{2.5}$ concentrations for the period 2000-2017 were derived from a series of model runs, in which sector emissions were individually reduced by 15%. An approximate contribution from that sector is then estimated by subtracting the reduction run from the base run (without sectoral emission reductions) and multiplying 100/15. The following sectors are

considered: traffic, industry, residential heating and agriculture. In addition, the contributions to PM_{10} and $PM_{2.5}$ from natural sources (i.e. sea spray and windblown dust) are distinguished. Further details are described in the EMEP Status reports (EMEP, 2018, 2019).

2.3 Observations

Air quality monitoring data from EEA's databases for the period 2000-2017, i.e. Airbase for data before 2013 and e-Reporting for data from 2013 and onwards, were extracted by April 2019. All data were compiled into daily data; for PM ad NO_2 we used daily averages whereas for O_3 we used MDA8 (the maximum daily 8 h running mean values). For NO_2, O_3 and PM_{10} we used the data capture criteria as given above, whereas for $PM_{2.5}$ this was relaxed to 65 %. PM could be measured both as hourly data and as daily samples. In the station's time series, we did not merge these data in the cases of a switch from e.g. daily to hourly sampling over the period so that annual mean can be computed either from daily or hourly values.

Only background sites were considered (i.e. excluding traffic and industrial stations), but no screening on the basis of altitude was performed considering that their influence on the overall results would be marginal, although models are not expected to be adapted to capture their specificities.

It should be emphasized that the completeness criteria led to select only measurement stations operating over a long period of time subsequently drastically reducing the spatial coverage. The conclusions of the present report only apply to a very limited subset of European stations. The discussion on model ability to capture the variability is therefore only relevant for those areas and not representative of overall model performances.

The EMEP observation data are all downloaded from the EBAS database infrastructure (http://ebas.nilu.no/) and aggregated to annual mean concentrations. Years with data coverage higher than 75% are included and time series with at least 14 years of data for the period 2000-2018 are used for trend analysis. Minor manual screening of the data has been done, i.e. obviously erroneous data are excluded. Time series from some sites which have moved a short distance have been merged, i.e. Birkenes/Birkenes II (NO0001R/NO0002R), Rörvik/Råö (SE0002R/SE0014R), Aspvreten/Norunda Stenen (SE0012R/ SE0022R), Vavihil/Hallahus (SE0011R/ SE0020R) , Virolahti II/Virolahti III (FI0017R/ FI0018R).

2.4 Trend calculations

The trend calculations on EMEP observations and model results were done on annual mean concentrations and were based on the Mann Kendall (MK) method for identifying significant trends combined with the Sen's slope method for estimating slopes and confidence intervals. These methods were programmed and run in Python using the pyMannKendall package (Hussain and Mahmud, 2019). Trends are considered statistically significant when the p-value of their Mann-Kendall statistic is lower than 0.05.

3 Validation

Both approaches experimented here are models, which require some form of validation. Since the statistical GAM model is fitted to the observation, it is unbiased by construction whereas the CTM may have a systematic bias. Similarly, the GAM also accounts for the long-term trend in the regression, so that the interannual long term evolution is also unbiased. Looking at the temporal correlation constitutes a more fair comparison, which is also justified since our focus here is on the capacity of such models to capture the extent to which they are able to represent the impact of meteorological variability on air quality evolution.

Since the focus is on long term trends, it is mainly the inter-annual correlation that we want to compare. But models are more classically assessed focusing on their day-to-day variability, so that we also discuss intra-annual correlations.

We focus first on intra-annual correlations. The correlation between modelled and observed daily indicators is computed for each year over the 2000-2017 period, and the median of the correlations found for each year is displayed as maps and scatter plot between the GAM and CTM models. Then we compare inter-annual correlations. Here we compute the correlation between the modelled and observed annual indicators over the period 2000-2017.For both types of correlations, a value close to one indicates the best performances.

3.1 Ozone

For ozone, we used MDA8 between April and September as a daily indicator, showing in Figure 1 only rural stations (other station types available in supplementary material). The GAM exhibits a slightly better capacity to capturing the day-to-day variability. Both models perform less well in southern Europe, which is a concern given the importance of ozone pollution there. The CTM performs less well as coastal sites in UK, Benelux, North of Germany and Scandinavia, presumably because of local meteorological features. The synthetic view in the scatter plot of Figure 2 confirms the overall better performance of the GAM, although both models remain fairly similar.

Figure 1: Intra-annual correlation between model (Left: CTM, right: GAM) and rural background observations (daily MDA8 from April and September). The correlations are computed for each year between 2000 and 2017, and the median over all year is plotted.

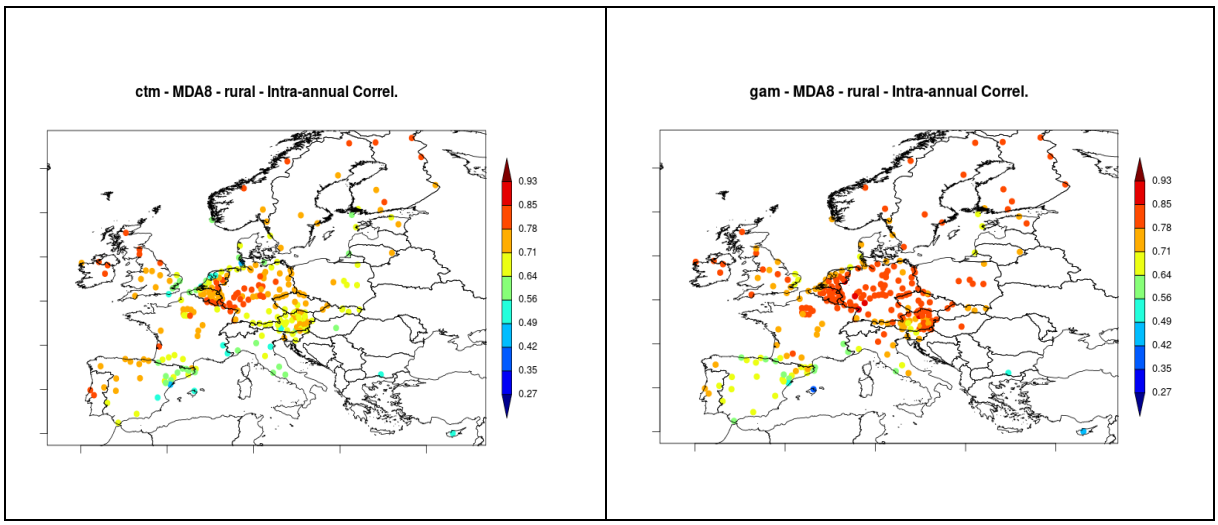

Figure 2: Scatterplot comparing GAM and CTM intra-annual correlations at rural background sites for daily MDA8 from April and September. The correlations are computed for each year between 2000 and 2017, and the median over all year is plotted.

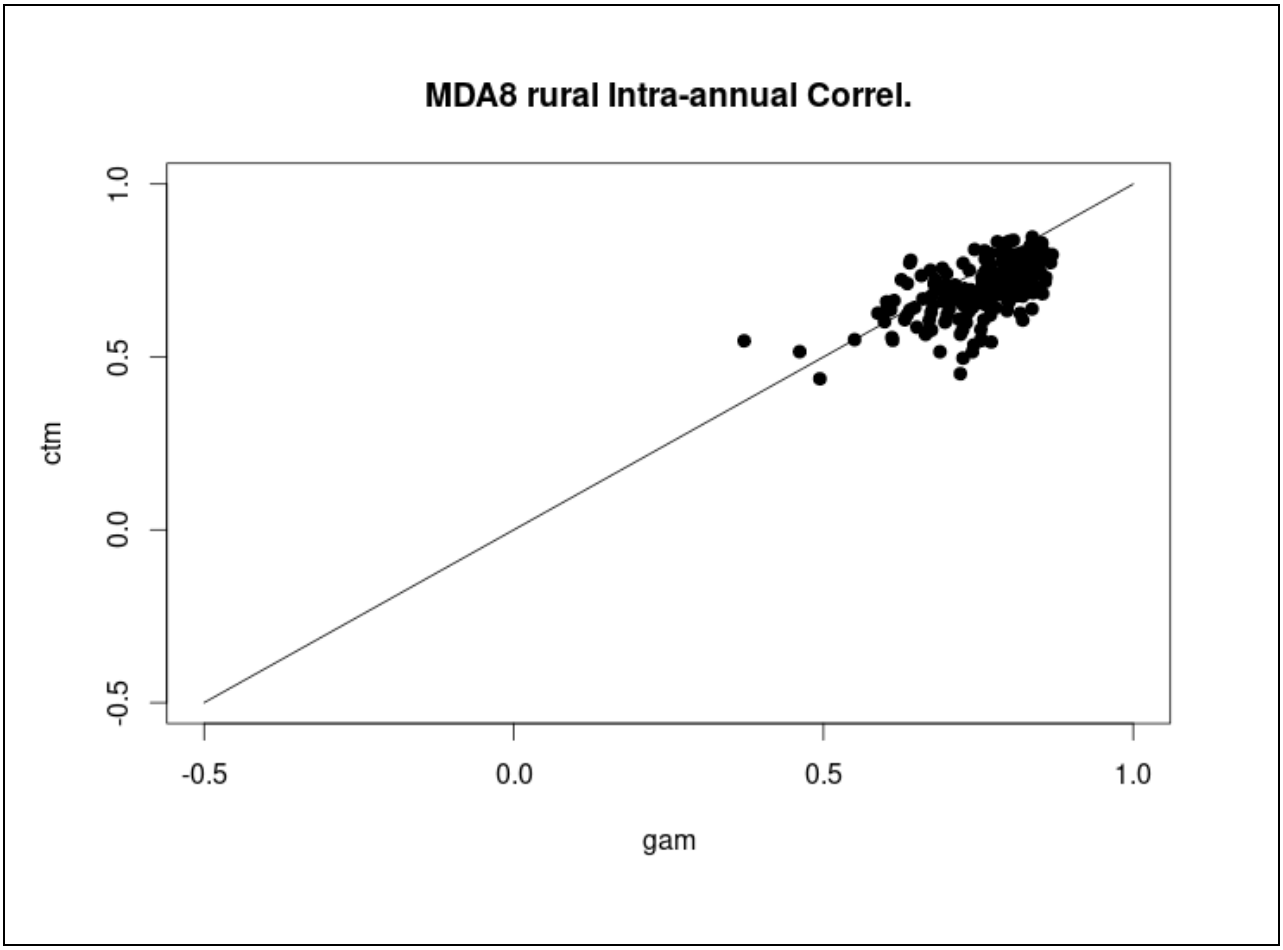

Since we are primarily interested to the long-term impact of meteorological variability on the trend, the essential feature to be captured by the models is the year to year variability. Inter-annual correlations are displayed in Figure 3 for the GAM and CTM, and for either the 4MDA8 (the fourth highest ozone peak – as daily maximum of the 8hr running mean - in a given year) and the average of MDA8 over April-September. For 4MAD8, both models have quite similar skill according to the scatterplot in Figure 4. Again, it is over Southern Europe that they perform less well. For the April-Sept. average of MDA8, the GAM model performs better in general (including over central Europe), there are improvement in southern Europe, although the correlations are still limited.

Figure 3: Inter-annual correlation between model (Left: CTM, right: GAM) and rural background observations (daily MDA8 from April and September). The correlations are computed over the 2000-2017 period for 4MDA8 (top) and the average of MDA8 between April and September (bottom).

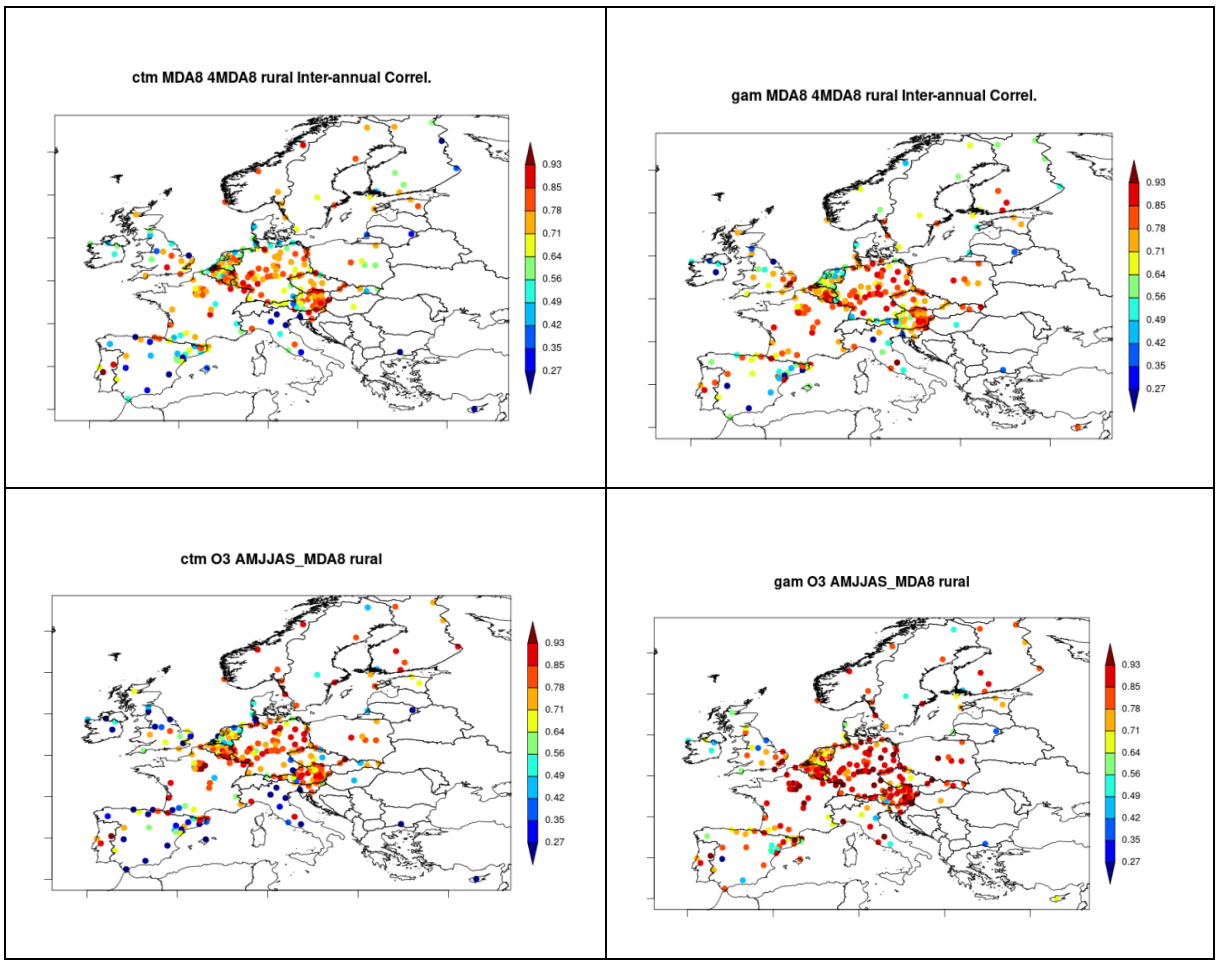

Figure 4: Scatterplot comparing GAM and CTM inter-annual correlations at rural background sites for 4MDA8 (left) and April-Sept. average of MDA8 (right). The correlations are computed for each year between 2000 and 2017, and the median over all year is plotted.

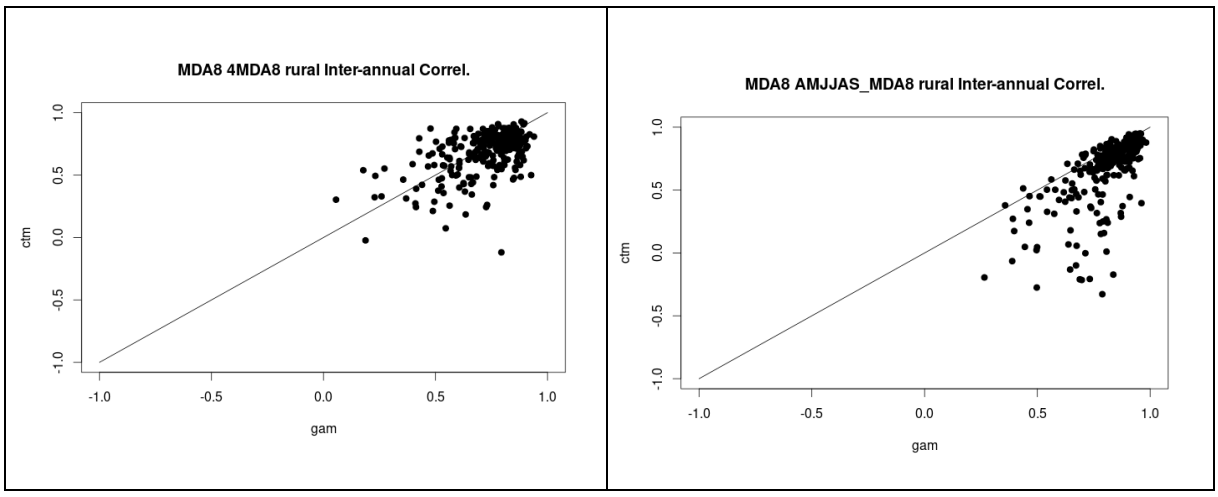

3.2 NO_2

The intra-annual correlation of the GAM model is notably better than that of the CTM for daily mean NO_2 as shown both in the map of correlation (Figure 5) and the scatterplot (Figure 6). The GAM model tends to perform better in urban sites, whereas on the contrary the CTM performs better at rural sites. The resolution of the EMEP model (10 km) implies that the grid values could not really be compared with measurements at urban locations, whereas on the contrary the GAM is specifically designed to capture local features. This difference in design has particularly strong impact for a short-lived pollutant as NO_2.

Figure 5: Intra-annual correlation between model (Left: CTM, right: GAM) and urban (top) and rural (bottom) background observations (based on daily NO_2). The correlations are computed for each year between 2000 and 2017, and the median over all year is plotted.

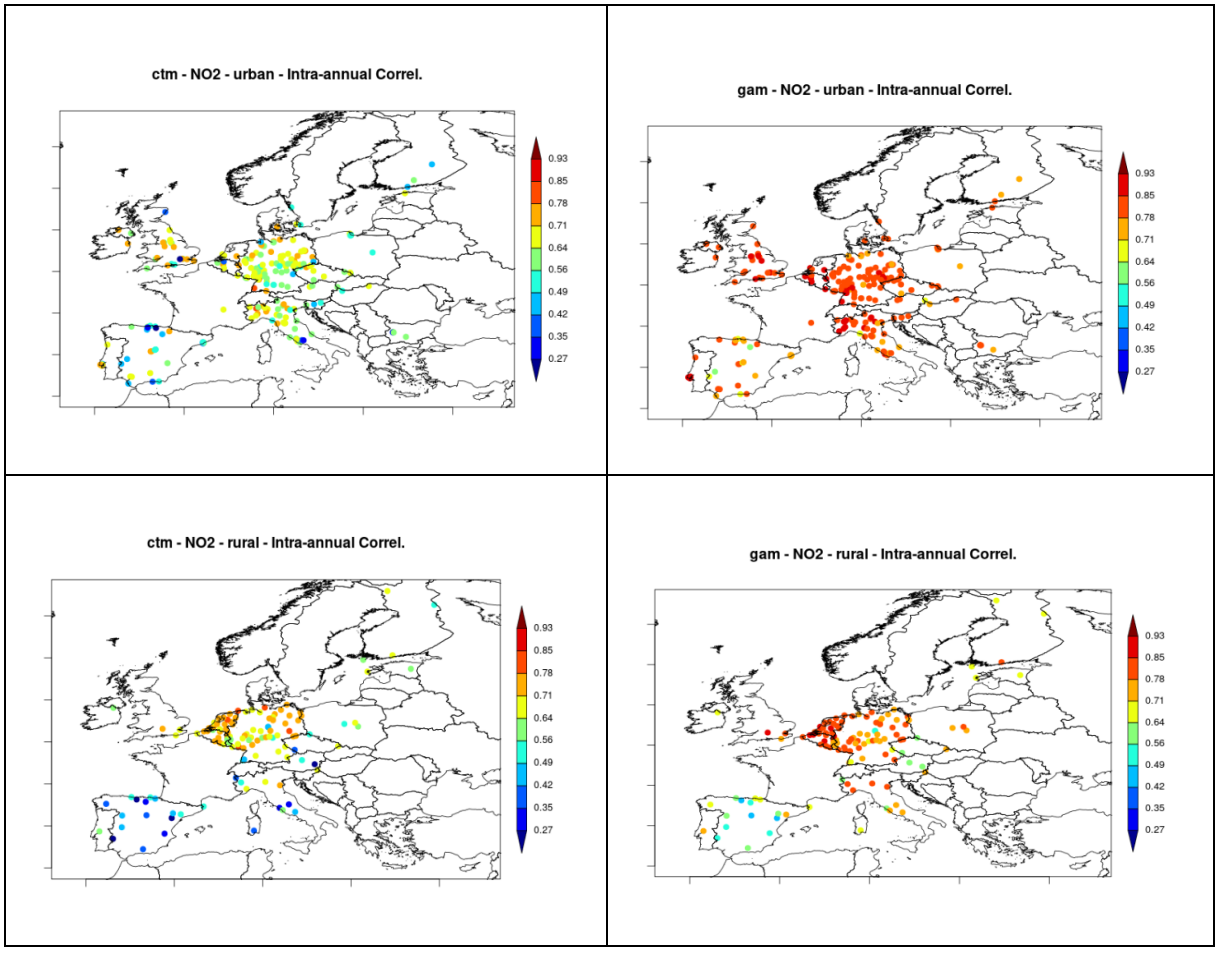

Figure 6: Scatterplot comparing GAM and CTM intra-annual correlations at urban (left) and rural (right) background sites for daily NO_2. The correlations are computed for each year between 2000 and 2017, and the median over all year is plotted.

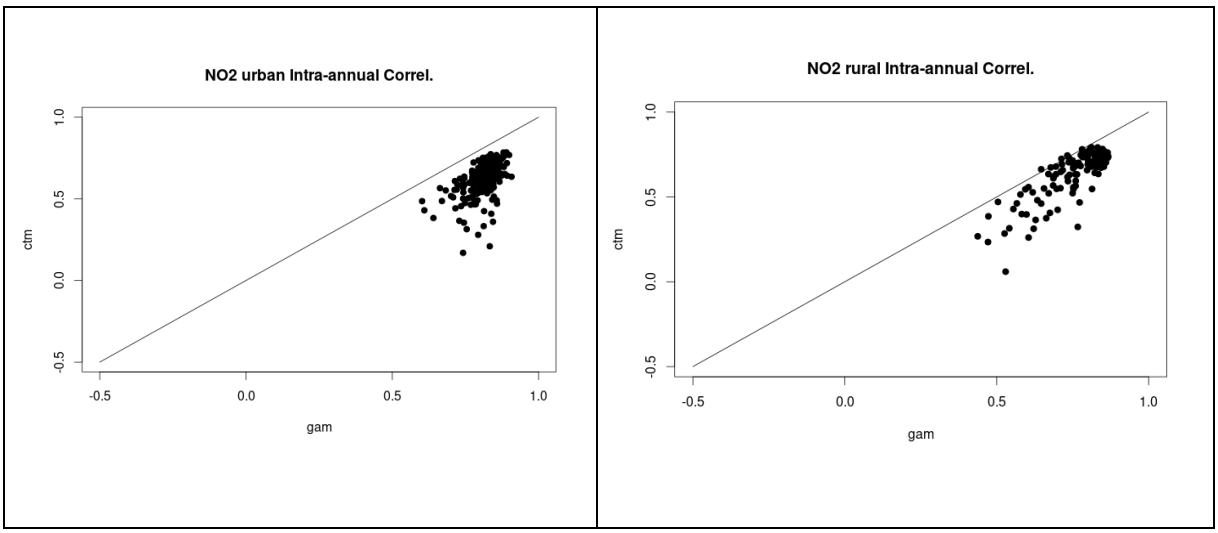

When it comes to inter-annual correlation, the performances of the CTM become closer, but are still surpassed by the GAM model (Figure 7 and Figure 8). There is a strong spatial variability in the performances of the CTM, for instance in Germany, Italy and southern Spain. Again, the discrepancy is larger at urban sites.

Figure 7: Inter-annual correlation between model (Left: CTM, right: GAM) and urban (top) and rural (bottom) background observations. The correlations are computed over the 2000-2017 period for annual mean NO_2.

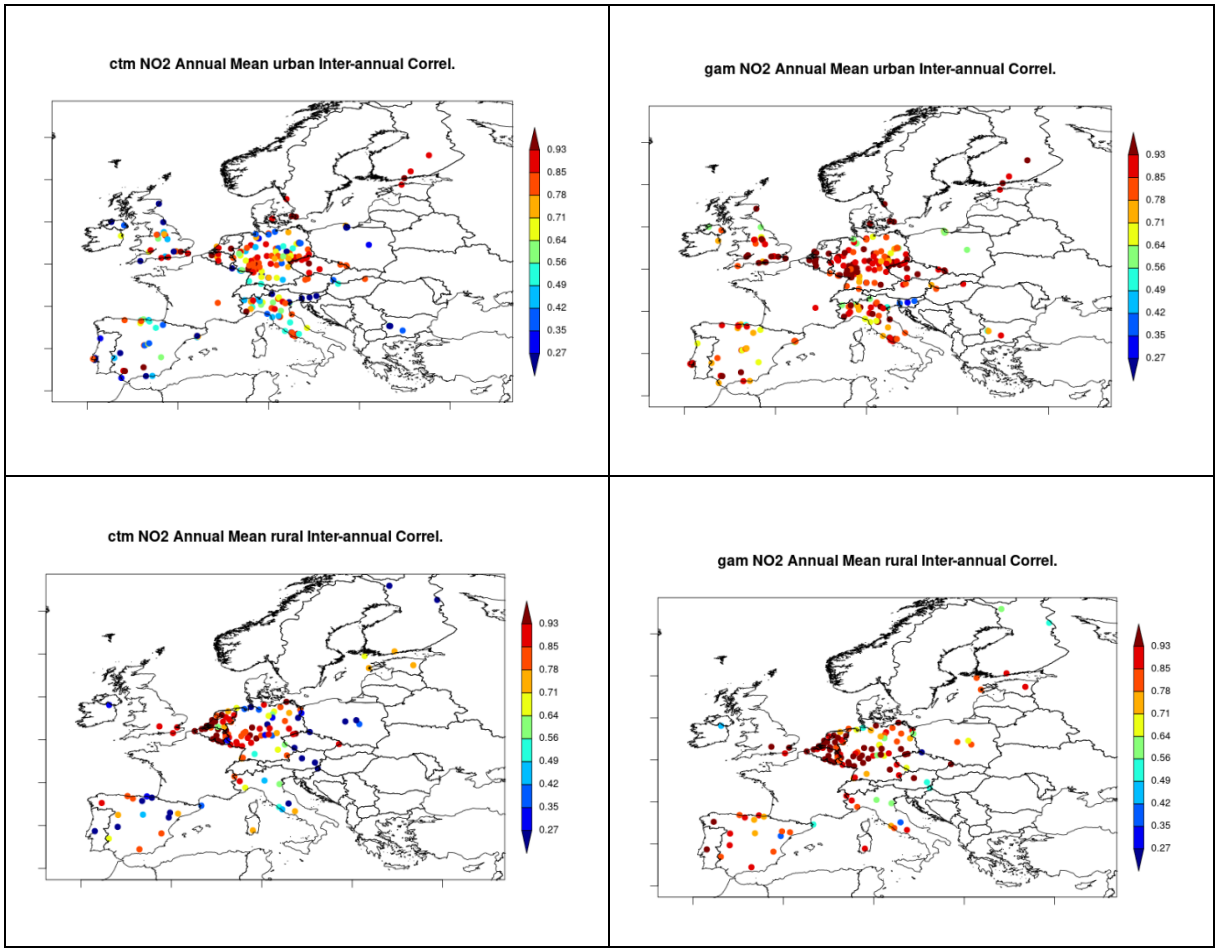

Figure 8: Scatterplot comparing GAM and CTM inter-annual correlations at urban (left) and rural (right) background sites for annual mean NO_2. The correlations are computed for each year between 2000 and 2017, and the median over all year is plotted.

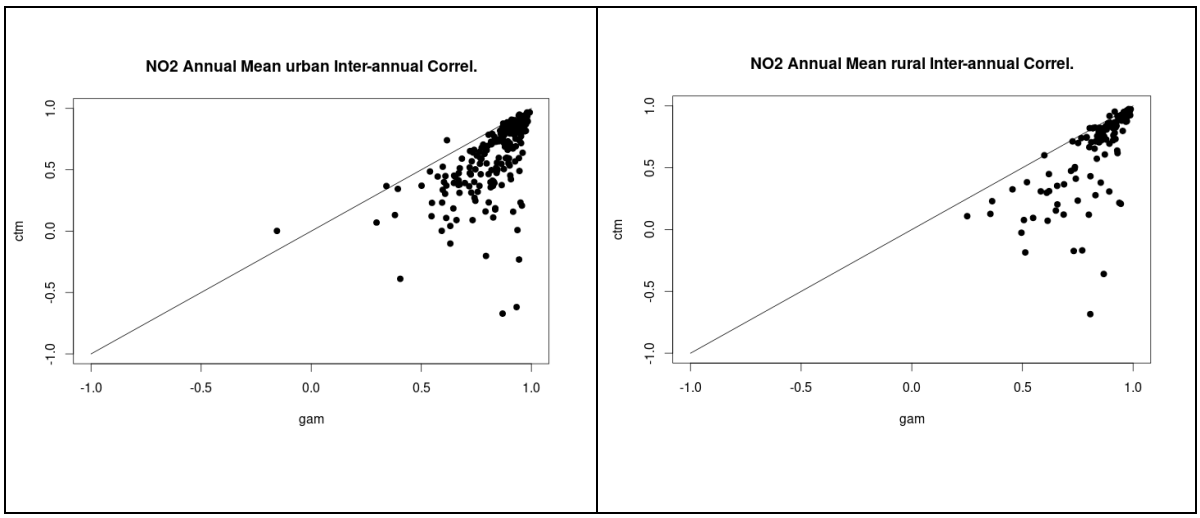

3.3 PM_{10}

The intra-annual correlations are lower for daily PM_{10} than NO_2 and MDA8, but better for the GAM model. The CTM performs less well throughout, but especially over Southern sites (Figure 9 and Figure 10).

Figure 9: Intra-annual correlation between model (Left: CTM, right: GAM) at urban (top) and rural (bottom) background observations (daily PM_{10}). The correlations are computed for each year between 2000 and 2017, and the median over all year is plotted.

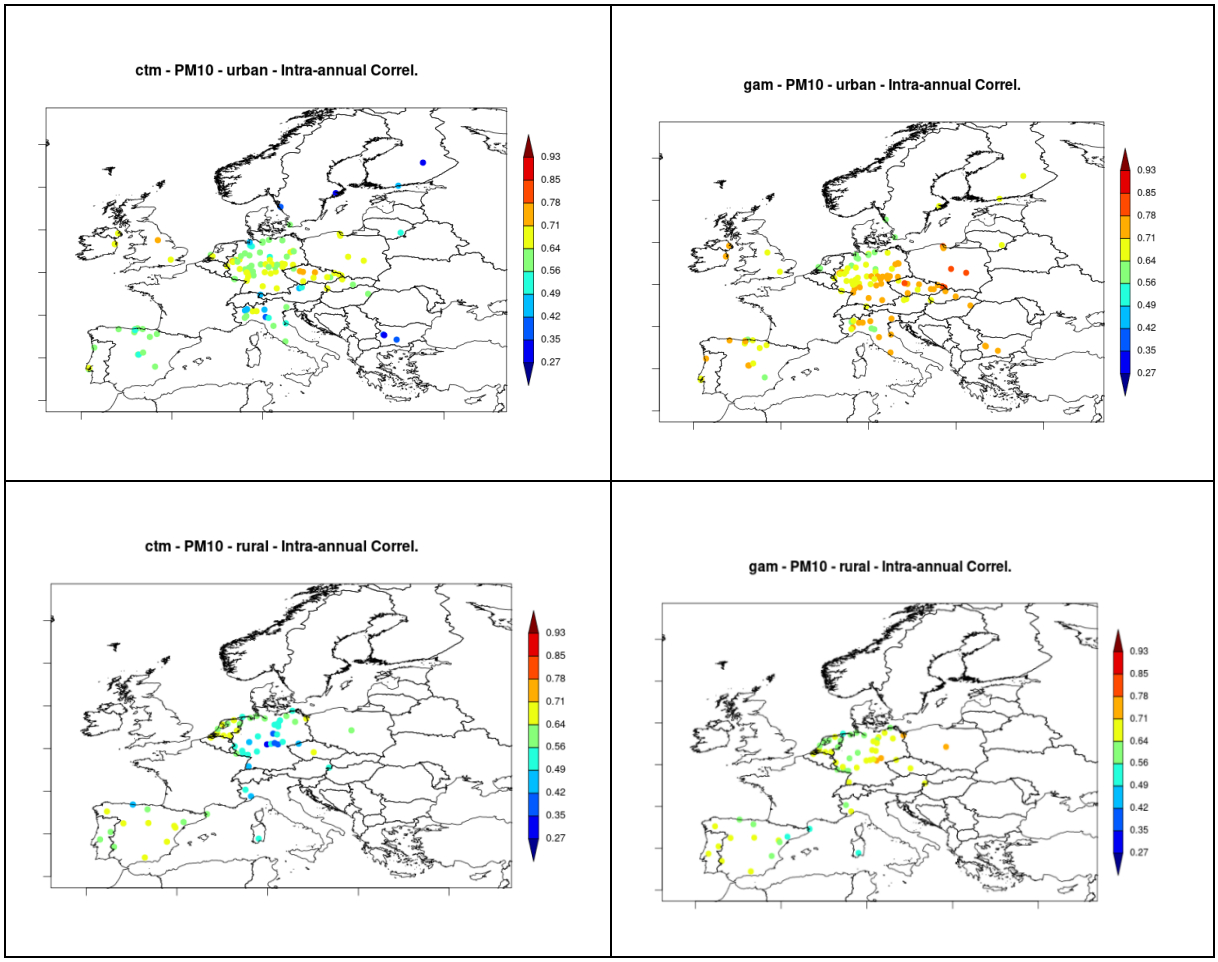

Figure 10: Scatterplot comparing GAM and CTM intra-annual correlations at urban (left) and rural (right) background sites for daily PM_{10}. The correlations are computed for each year between 2000 and 2017, and the median over all year is plotted.

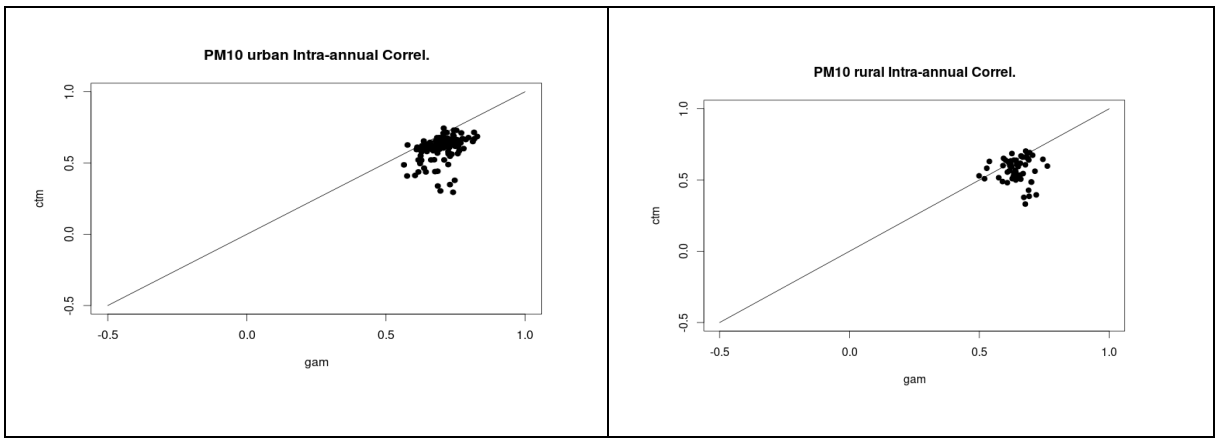

As mentioned in section 2.3, the completeness criteria applied to select long-term stations lead to reduce drastically the dataset, so that the intra-annual correlation should not be interpreted in terms of overall model performances. To further illustrate that, we show in Figure 11 the intra-annual correlation of the EMEP MSC-W model for all stations available for a recent year (2017). The correlations are there much better than over the reduced dataset presented in Figure 9.

Figure 11: Intra-annual correlation between model and background observations (daily PM_{10}) at rural (left) and urban (right) sites . The correlations are computed for the year 2017.

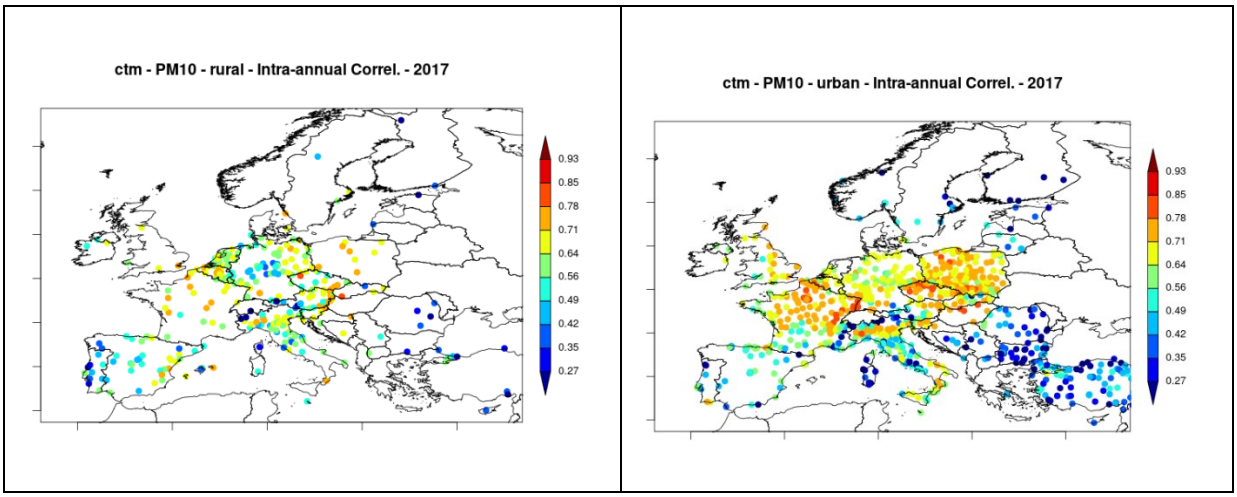

The performances are better for the inter-annual correlation (Figure 12 and Figure 13). The GAM model still performs better but to a lesser extent, except at a few scattered sites where the improvement is notable.

Figure 12: Inter-annual correlation between model (Left: CTM, right: GAM) at urban (top) and rural (bottom) background observations. The correlations are computed over the 2000-2017 period for annual mean PM_{10}.

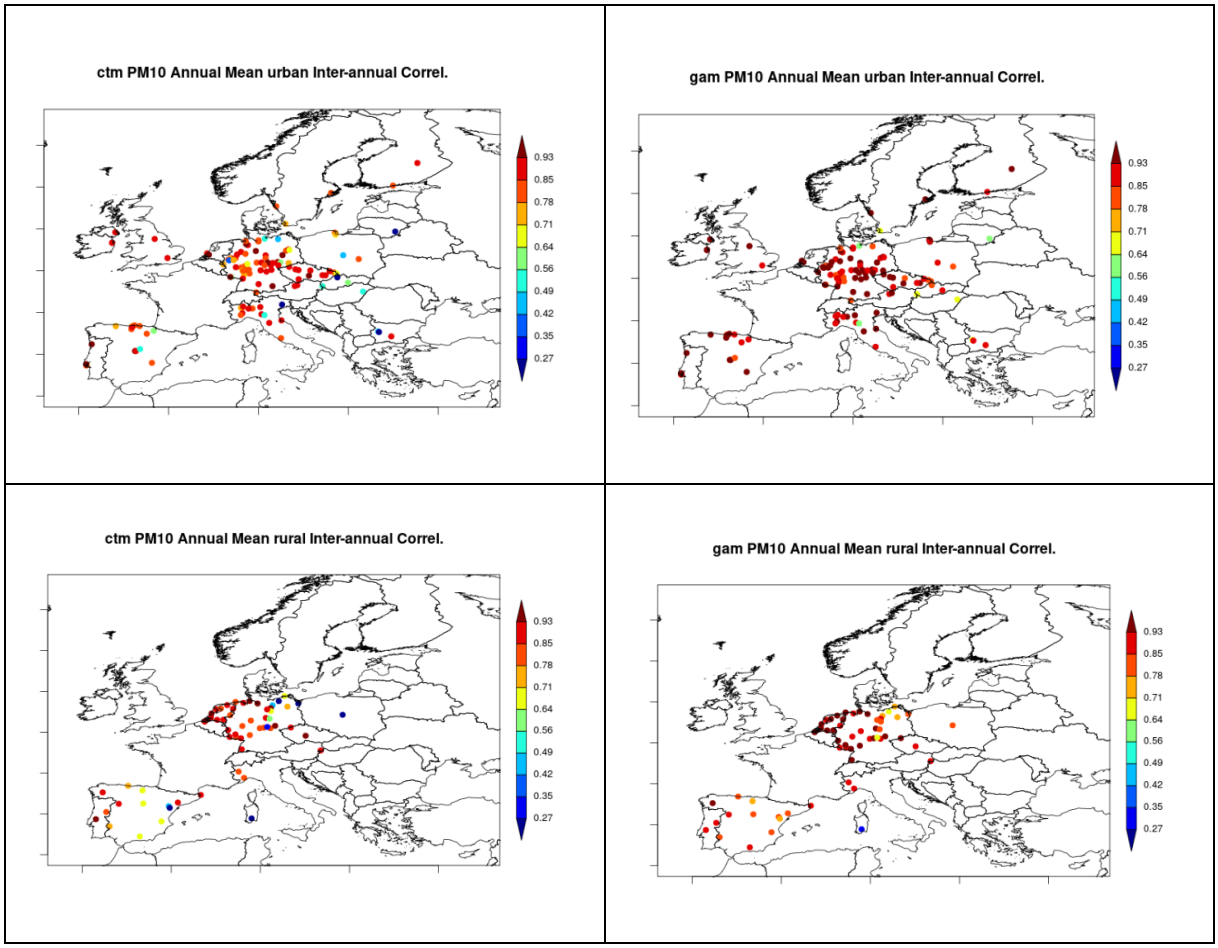

Figure 13: Scatterplot comparing GAM and CTM inter-annual correlations at urban (left) and rural (right) background sites for annual mean PM_{10}. The correlations are computed for each year between 2000 and 2017, and the median over all year is plotted.

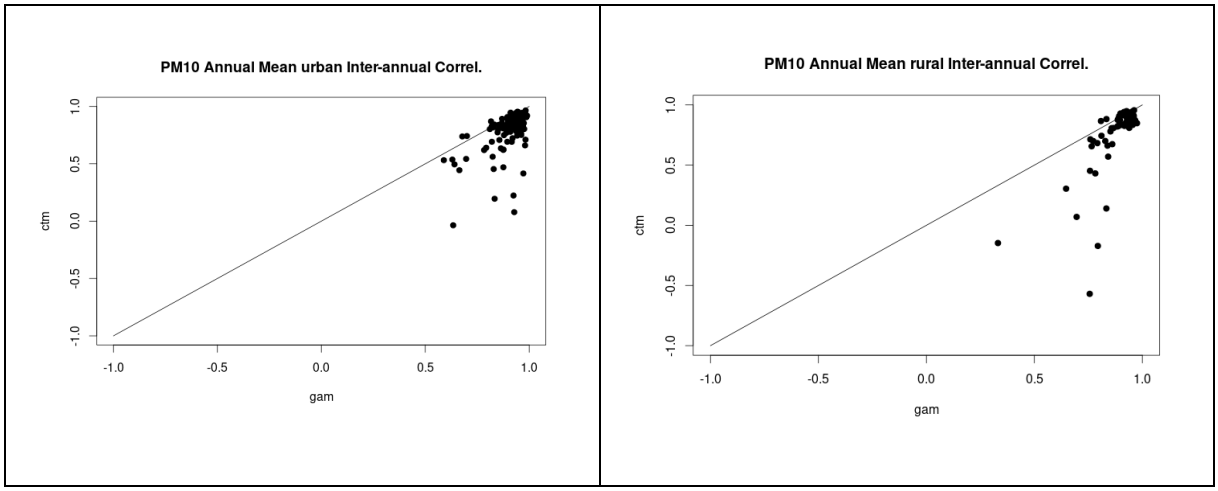

4 Results

4.1 Meteorological decomposition

4.1.1 Time series 2000-2017

Here we compare the Europe-wide median of interpolated time series at individual stations for either the CTM or GAM model. For both models, we display the time series of the reference simulation and the time series of a sensitivity scenario where only meteorological variability is targeted. These comparisons are not intended to assess the biases of the models. Such biases are out of the focus of the present study because: (i) they are not informative with regards to the effect of meteorological variability on air quality, (ii) they are of a totally different nature between the CTM and GAM models so that no fair comparison can be proposed.

For ozone (as 4MDA8), the time series in Figure 14 confirms that the interannual variability is too low in the CTM where outstanding years such as the 2003 heatwave are less pronounced than in the GAM.

Figure 14: Median over Europe for 4MDA8 at urban (red), suburban (blue) and rural (green) background sites in the observation (solid lines with open circles), the models (solid) and the model excluding long term trend (dotted lines) (CTM: top, GAM: bottom)

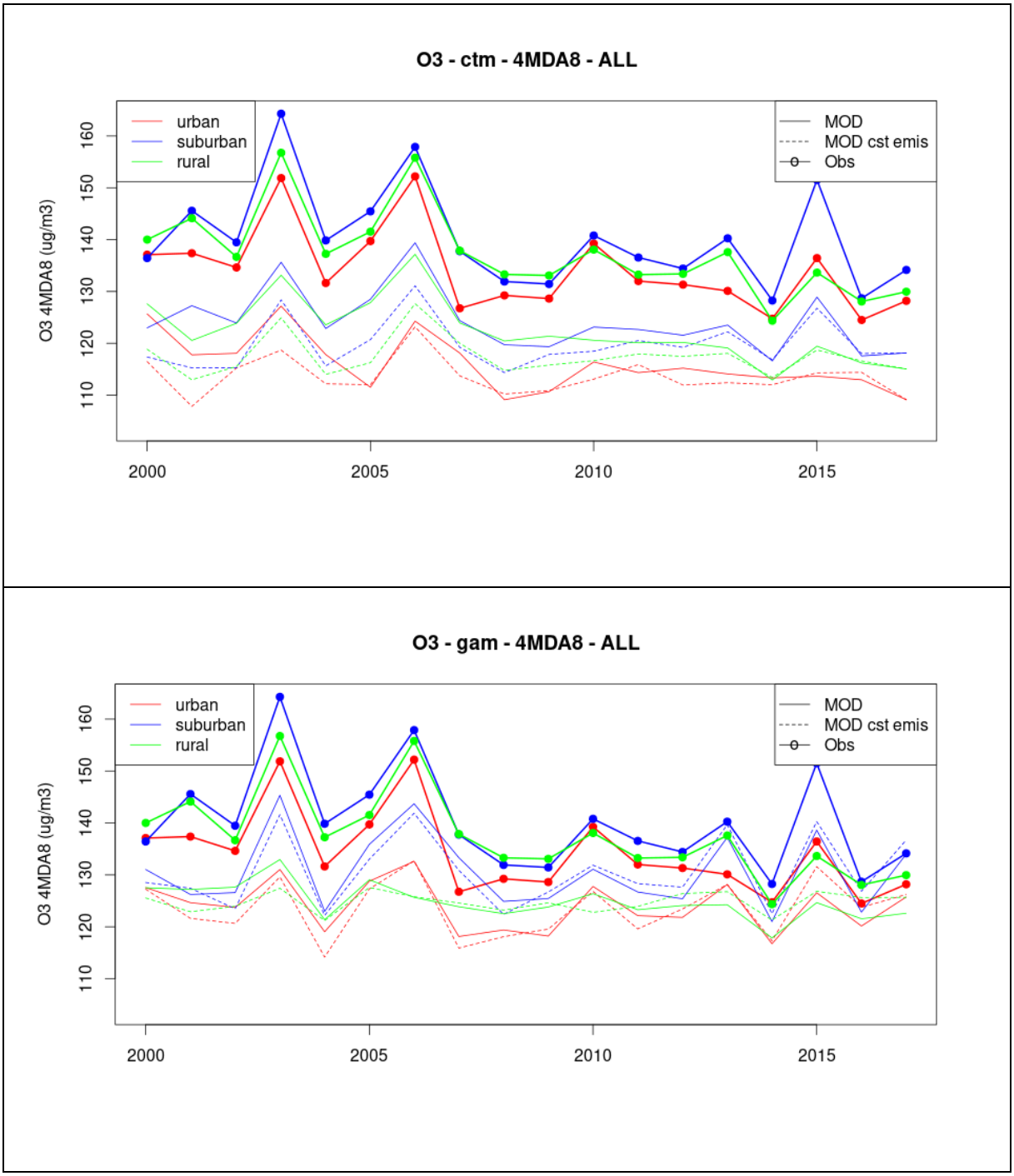

For NO_2, the interannual variability is much lower than for ozone (Figure 15). The comparison between CTM and GAM is not entirely fair as the GAM is unbiased by design (including for the long-term trend, which is fitted on observations). Therefore, we also provide in Figure 15, the normalized trends (based on 2000 concentrations), where the comparison is more fair to demonstrated the limited interannual variability in the CTM compared to the GAM.

Figure 15: Median over Europe for NO_2 annual mean at urban (red), suburban (blue) and rural (green) background sites in the observation (solid lines with open circles), the models (solid) and the model excluding long term trend (dotted lines) (CTM: top, GAM: bottom). The timeseries normalized to 2000 concentrations (in %) are displayed in the right-hand side column.

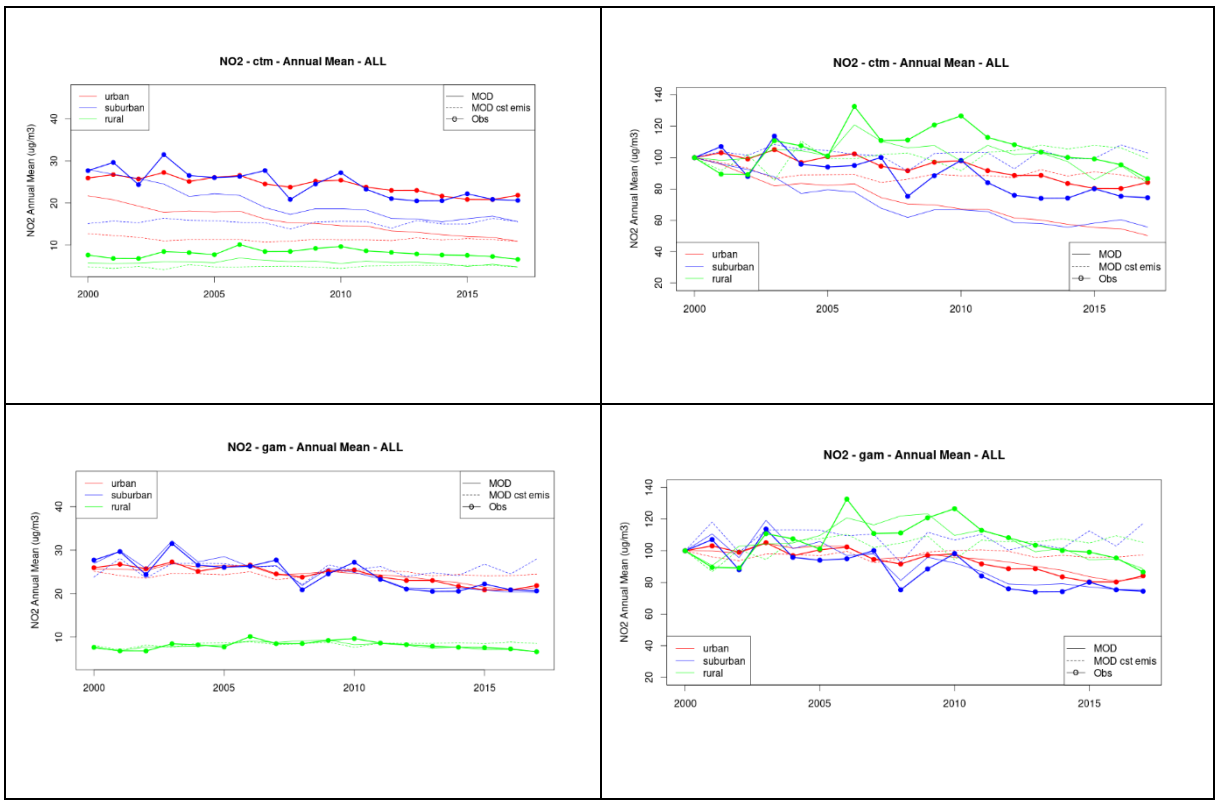

For PM_{10}, the bias of the CTM also precludes a direct comparison of the time series with the GAM, so that relative trends are also shown in Figure 16. Here the interannual variability appears visually more in-line with observations compared to the GAM.

Figure 16: Median over Europe for PM_{10} annual mean at urban (red), suburban (blue) and rural (green) background sites in the observation (solid lines with open circles), the models (solid) and the model excluding long term trend (dotted lines) (CTM: top, GAM: bottom). The timeseries normalized to 2000 concentrations (in %) are displayed in the right-hand side column.

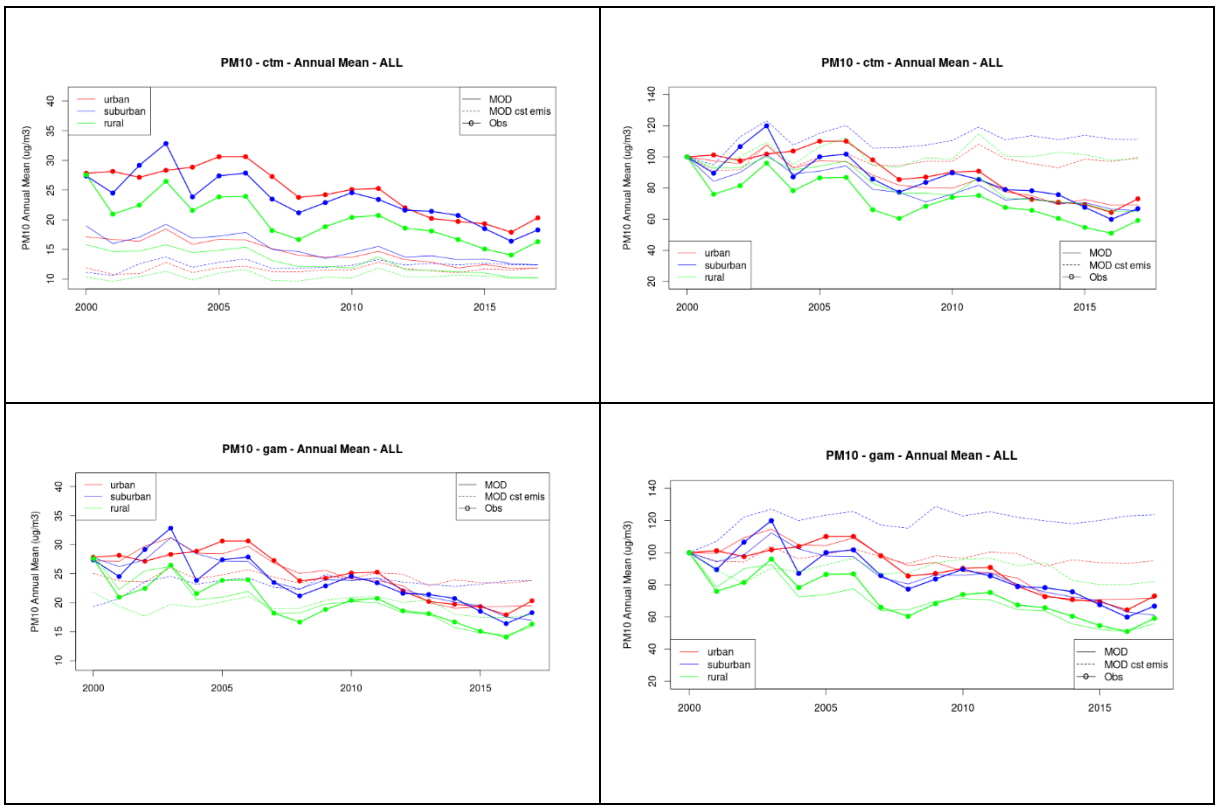

4.1.2 Interannual variability due to meteorology and other factors.

For both the GAM and CTM, we present here the median trend by country for rural sites with a decomposition of the main drivers.

For the CTM, the decomposition is based on the difference between a reference simulation (where emission, meteorology and boundary conditions change from year to year) and a sensitivity simulation (where only emissions are kept constant). With such a combination, it is possible to isolate (1) the impact of emissions, (2) the impact of meteorology and the background (boundary conditions).

The GAM is trained on the basis of a determined set of predictors including daily meteorological parameters and a long-term coefficient. This long-term coefficient is considered to capture both annual emission and background changes. We will therefore consider that for the GAM, the decomposition be considered to isolate (1) the impact of meteorology and (2) the impact of emissions and background.

For both the CTM and GAM time series over 2000-2017, we then compute linear trend over the whole period using the Sen-Theil Slope.

The main limiting factor for the comparison of CTM and GAM results is therefore the fact that the decomposition is not strictly representing the same factors. Such a discrepancy in the methodological approach is expected to be important for O_3, marginally important for PM, and negligible for NO_2.

Ozone

The median trend by country is reported in Figure 17 for both the CTM and GAM result and indicating the importance of the main contributing factors.

For rural sites, we identify decreases for all countries and both the highest peaks (4MDA8) and summertime average of the peaks (AMJJAS average of daily MDA8). A quite robust finding is that the effect of emission changes dominates in all countries, for both ozone metrics, and for both GAM and CTM results. The impact of the meteorological factor appears larger for 4MDA8 compared to the April-Sept. average of MDA8 in both the GAM and the CTM. There is however a clear discrepancy between both models, with the CTM indicating systematic declining trends due to the meteorological & background factor, whereas the GAM indicates some increases regarding the effect of meteorology alone. This difference is attributed to a compensation brought about by background ozone, as boundary conditions in the CTM contribute to a decreasing trend. With the model setup used here, it was not possible to disentangle meteorology and background factors, although refining this could be solved by an additional model sensitivity simulation isolating both effects.

With the GAM, the impact of the meteorology alone can be identified, and it appears to have contributed to increase 4MDA8 trends in AT, BE, CZ, DE, FR, IT, and the European average. The quantitative trends by country and the relevant factor decomposition are also reported in Table 1. For the GAM, this table also include the ratio between the trend due to meteorology versus other factors (in %). For Austria, Belgium, Czech Republic, France, and Italy meteorological variability between 2000 and 2017 counter-acted the reduction brought about by emission and background changes by a magnitude ranging between 20 and 40 % the magnitude of emission reductions, for Italy the magnitude is even almost 80%. On the contrary, for the Netherlands, Norway, and Sweden, meteorology contributed to further decrease the trend by 30 to 50% the magnitude of emission reductions. In the CTM the meteorology and background factors are merged, and we find that they contributed to further reinforce downward trends of 4MDA8 by 20 to 150% the magnitude of emission impact in Belgium, Finland, France, Great Britain, Norway, Poland, Portugal, The Netherlands, Sweden and Slovakia.

Figure 17: Decomposition of the driving factors: emission (blue) versus meteorology and background (green) for the CTM (left) and emission and background (blue) versus meteorology (green) GAM (right) and 4MDA8 (top) and April-Sept. MDA8 average (bottom) at rural background sites. For each country we provide in parenthesis: the number of stations, the median interannual correlation. The red stars indicate the sum of both factors.

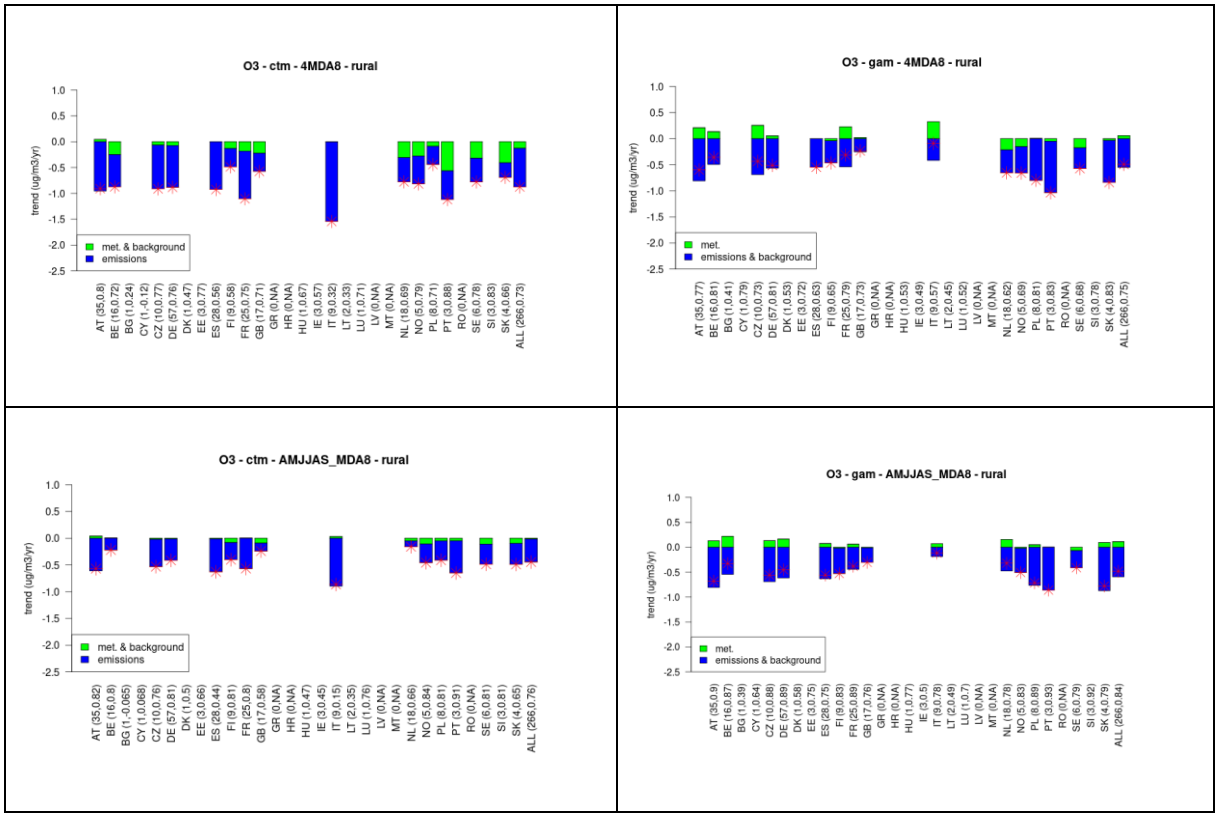

Table 1: Trend by country and for all the domain for 4MDA8 over 2000 and 2017 in the CTM and GAM model and decomposition of the meteorological, emission and background factors (in µg/m3/year) as well as relative proportion of meteorology (and background for the CTM) and emissions (and background for the GAM) in %, negative when opposite in sign.

	CTM				GAM			
	Met & Bkgd (µg/m3/yr)	Emis (µg/m3/yr)	Net trend (µg/m3/yr)	Met & Bkgd / Emis (%)	Met (µg/m3/yr)	Emis & Bkgd (µg/m3/yr)	Net trend (µg/m3/yr)	Met / Emis & bkgd (%)
AT	0,05	-0,95	-0,91	-4,8	0,21	-0,81	-0,60	-25,9
BE	-0,25	-0,62	-0,87	40,0	0,14	-0,49	-0,36	-27,4
CZ	-0,06	-0,85	-0,91	7,6	0,26	-0,69	-0,43	-37,1
DE	-0,07	-0,81	-0,88	9,1	0,05	-0,57	-0,51	-9,5
ES	0,00	-0,92	-0,93	0,0	0,00	-0,55	-0,55	0,4
FI	-0,13	-0,36	-0,49	36,8	-0,04	-0,42	-0,46	9,5
FR	-0,18	-0,92	-1,10	19,9	0,23	-0,54	-0,31	-42,2
GB	-0,22	-0,35	-0,58	62,8	0,02	-0,25	-0,23	-8,0
IT	0,00	-1,54	-1,54	0,2	0,33	-0,42	-0,09	-78,4
NL	-0,31	-0,47	-0,78	65,3	-0,21	-0,44	-0,65	49,0
NO	-0,28	-0,54	-0,82	51,3	-0,15	-0,51	-0,66	30,2
PL	-0,09	-0,35	-0,44	25,0	0,01	-0,80	-0,80	-0,8
PT	-0,56	-0,56	-1,12	101,5	-0,05	-0,99	-1,04	5,0
SE	-0,32	-0,46	-0,78	69,0	-0,17	-0,40	-0,57	44,0
SK	-0,41	-0,28	-0,69	144,5	-0,03	-0,81	-0,84	4,1
ALL	-0,13	-0,75	-0,87	17,0	0,06	-0,55	-0,49	-10,6

In the maps of Figure 18, it appears that the increase attributed to meteorology in the GAM is strongest in Western Europe, especially for the April-Sept. average of MDA8. There are also increases in Spain and Italy, but in these countries, there is also a substantial variability depending on the stations.

Figure 18: Maps of the trend (µg/m^3/yr) of 4MDA8 (top) and April-Sept. MDA8 average (bottom) at rural sites attributed to meteorology and background changes in the CTM (left) and meteorology in the GAM (right)

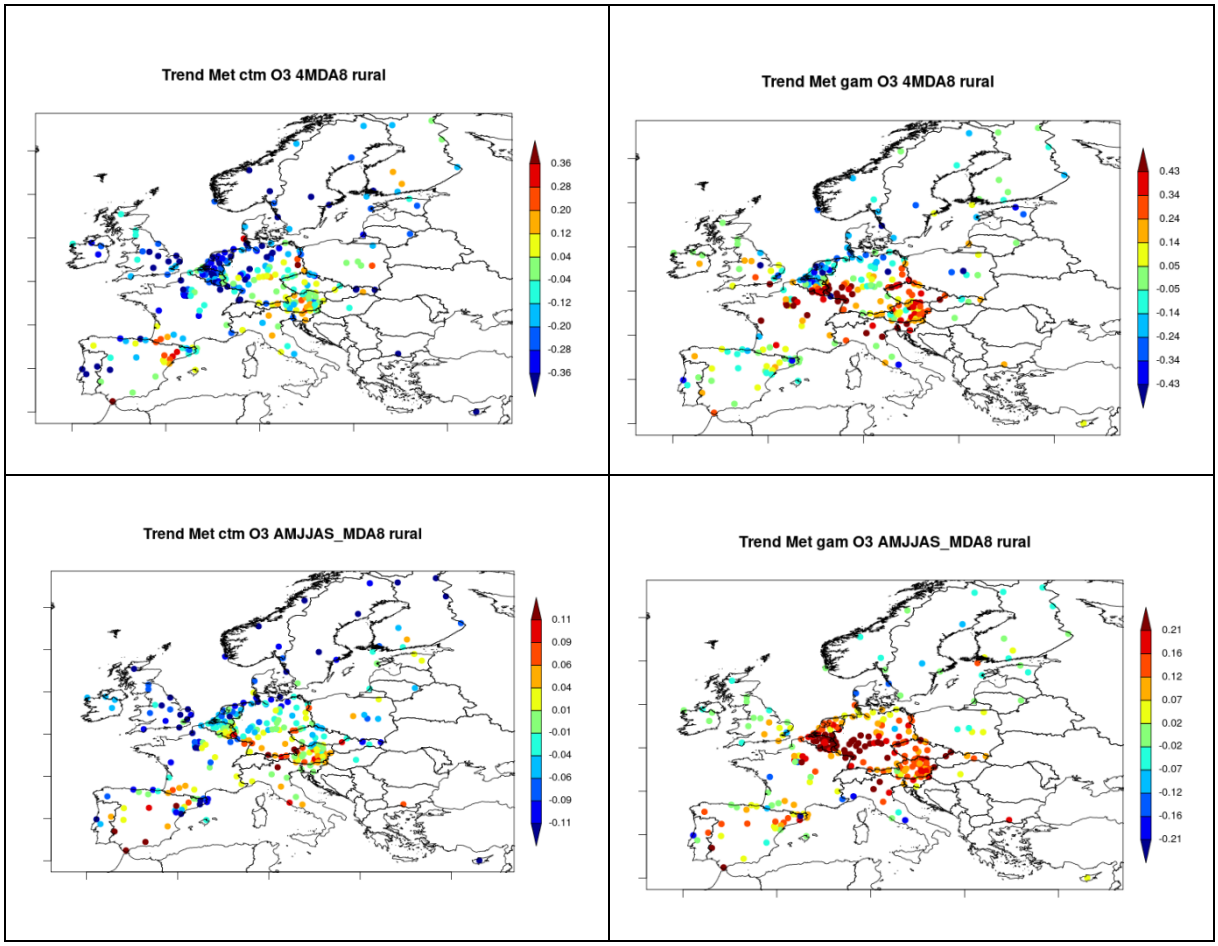

NO_2

For NO_2, the GAM and CTM are very consistent in concluding that the meteorology and background factor have very little impact (Figure 19), even if the estimate of the trend itself can differ between both models.

Figure 19: Decomposition of the driving factors: emission (blue) versus meteorology and background (green) for the CTM (left) and emission and background (blue) versus meteorology (green) GAM (right) for annual mean NO_2 at urban background sites. For each country we provide in parenthesis: the number of stations, the median interannual correlation. The red stars indicate the sum of both factors.

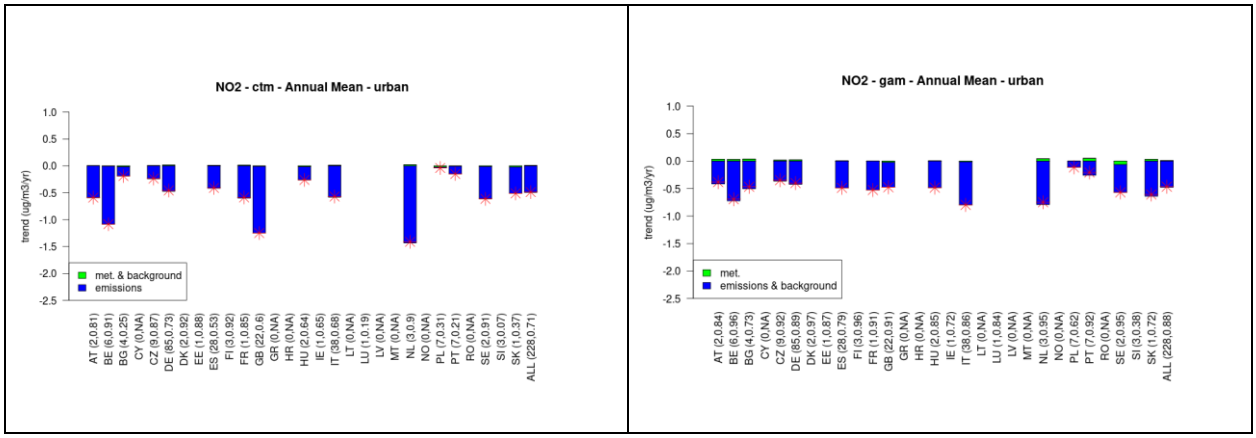

In the maps of Figure 20, there are also substantial increase of NO_2 attributed to meteorology, but those are very small compared to the overall trend.

Figure 20: Maps of the trend ($\mu g/m^3/yr$) of annual mean NO_2 attributed to meteorology and background changes in the CTM (left) and meteorology in the GAM (right)

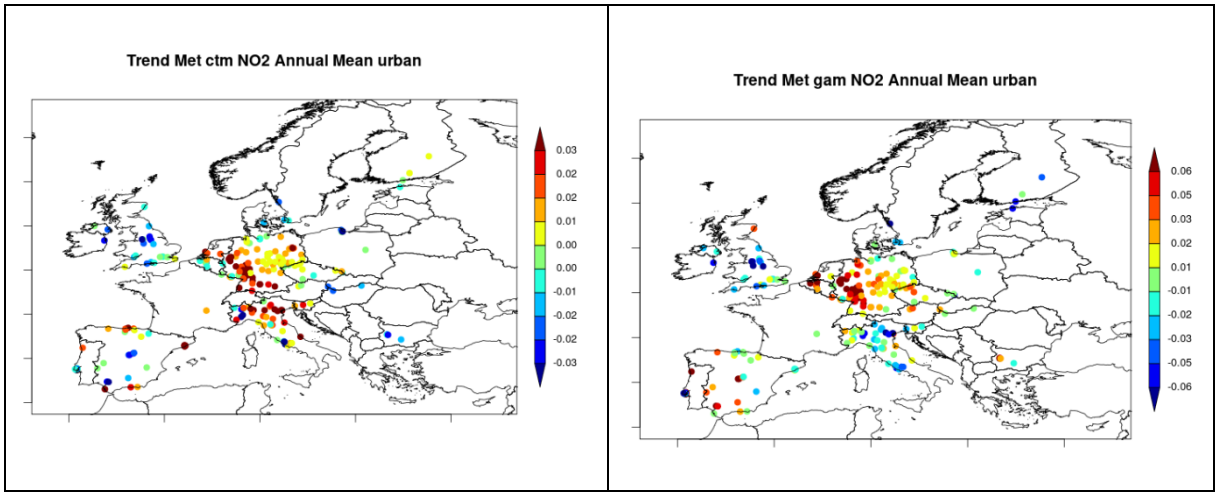

PM_{10}

For PM_{10} also the impact of the meteorological and background factor on the trend can be considered as negligible according to both the GAM and the CTM and for all countries (Figure 21).

Figure 21: Decomposition of the driving factors: emission (blue) versus meteorology and background (green) for the CTM (left) and emission and background (blue) versus meteorology (green) GAM (right) for annual mean PM_{10} at urban background sites. For each country we provide in parenthesis: the number of stations, the median interannual correlation. The red stars indicate the sum of both factors.

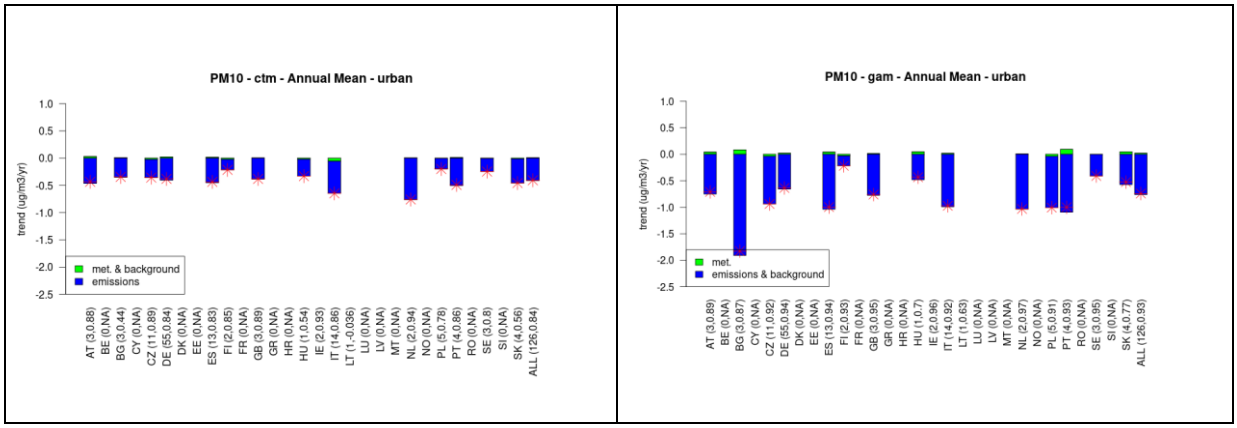

As for NO_2, in the maps of Figure 22, there are also substantial increase of PM_{10} attributed to meteorology, but those are very small compared to the overall trend.

Figure 22: Maps of the trend of annual mean PM_{10} attributed to meteorology and background changes in the CTM (left) and meteorology in the GAM (right)

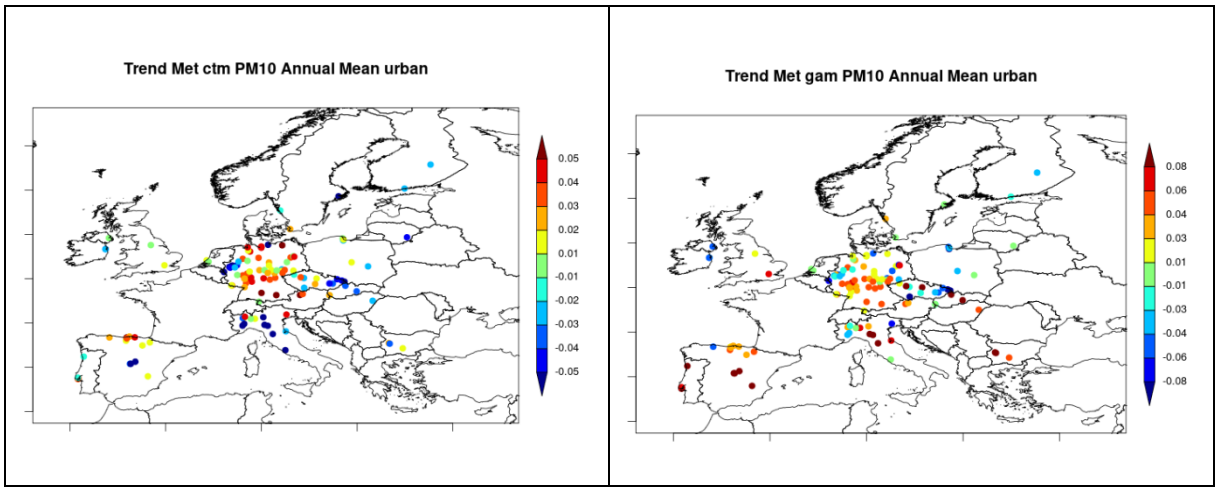

4.2 Precursor trends

In this section, we compare the trends of species that can be – in a first approximation – be related to emission of precursors (Figure 23).

We rely on both the comparison of time series (i) for concentrations at AQ e-reporting stations and primary emissions (also presented in a previous ETC report (Colette and Rouïl, 2020), and (ii) for concentration at EMEP sites and results of the EMEP MSC-W model. All results are presented relative to the levels in 2000. There are however a couple of minor differences in these figures that should not impair the comparison. The normalization is done towards unity with the exact 2000 value for EMEP, and towards 100% with the fitted value of the linear regression for AQ e-reporting. In addition, the

EU27+UK emissions are used in the comparison with EMEP data while only the countries hosting the selected sites are used in the comparison with AQ e-reporting data, both being extracted from EMEP Centre on Emission Inventories and Projections (https://www.ceip.at/data-viewer).

The emissions reductions of SOx are higher than we observe in the SO_2 measurements at both EMEP and AQ e-reporting sites. This larger decrease in emission also have an impact on the modelled concentrations which decrease faster than observations. A sharp decrease in emission was reported in 2008 and 2009 compared to the rate of decrease prior to 2007, this gain in reduced emission was maintained in following years. In the observed concentrations (both EMEP and AQ e-reporting sites) such a sudden decrease was found between 2006 and 2007, and it was not so pronounced in following years so that a substantial mismatch between emissions and concentrations (both modelled and observed) is found for more recent years.

A similar mismatch is also seen for NOx/NO_2 at AQ e-reporting sites after 2008. But at AQ e-reporting rural sites, the discrepancy tends to be reduced in later years. Likewise, a spike is seen in 2010 at EMEP sites, but the agreement is better in following years. One should note that most EMEP data are measured with manual method while for AQ e-reporting sites all are monitors. The monitors can have a positive bias from humidity and PAN, which may influence the observations in especially in rural areas. But this does not explain the main reason for difference between emissions and observations at urban, traffic and industrial AQ e-reporting sites.

Figure 23: Time series for concentration at EMEP sites and results of the EMEP MSC-W model and emissions from EU27+UK (left) and for concentrations at AQ e-reporting stations and primary emissions (right), for SOx/SO_2 (top) and NOx/NO_2 (bottom)

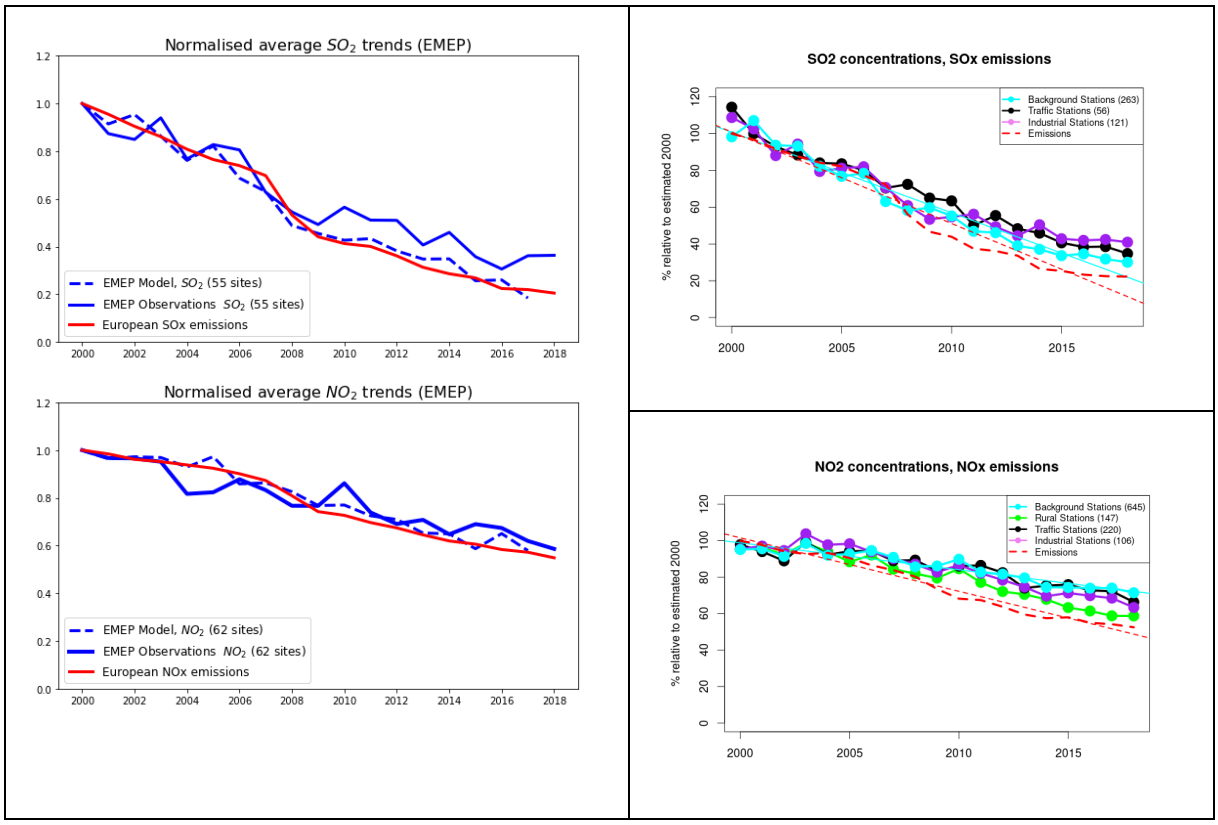

4.3 Trends in atmospheric composition

Trends in major precursor gases (SO_2 and NO_2) and the main constituents in aerosols are calculated on all available EMEP data. For the secondary inorganic aerosol (SIA) components (SO_4, NO_3, NH_4) this means mainly observations with filter pack sampler, which usually do not have any size specific cut off. Some observations are also in PM_{10}. SIA components in $PM_{2.5}$ are often only measured with one 24h sample per week, and these data are not included in the trend calculation. To calculate the trends in dust, measurements of iron (Fe) has been used as a tracer and multiplied with 100 to estimate the total dust concentration. For sea salt, observations of sodium (Na) has been used and multiplied by 2.5 to estimate the amount of total sea salt.

For organic carbon (OC) there are very few sites with long term consistent measurements, thus only observations from Birkenes (NO0002) and Ispra (IT0004) in $PM_{2.5}$ have been included. In PM_{10} there are also available data from Birkenes but these has not been included. For the interest of the reader, trends in organic aerosols at Birkenes has recently been published by (Yttri et al., 2020). Data from Ispra has been corrected prior to 2008 with a constant of 1.7 µg C/m^3 to adjust for the effect of installing a denuder in 2008.The analytical protocol changed at Birkenes in 2008 and at Ispra in 2005 and 2008, causing a change in the split between EC and OC, which will have an effect on the trends, particularly for EC, but this component has not been included in this analysis.

Figure 24 and Table 2 show trends in observations of aerosol species and precursor gases at EMEP sites compared with the EMEP MSC-W model result. The reductions in aerosol mass and SIA components are comparable between model and observations, especially in the changes in absolute concentrations. The relative change is somewhat higher for the model in PM_{10} and SO_4 (and SO_2) for the model compared to observations. There have been significant reductions in PM and SIA since 2000. Of the SIA components, it has been highest reductions in sulphate.

For organic aerosols there are too few sites to give a robust comparison, but the observations indicate a larger reduction in these components compared to what is found by the EMEP model. For the natural components dust and sea salt the observations indicate a reduction, but the variability is high and few sites show with significant trends.

Figure 24: Trends in inorganic precursor gases and aerosol chemistry at EMEP sites from 2000-2018 compared with EMEP MSC-W model results at the same sites for 2000-2017. The shaded area in the line plots indicate the 95% confidence interval. Box-whisker plots are given for absolute and relative trends

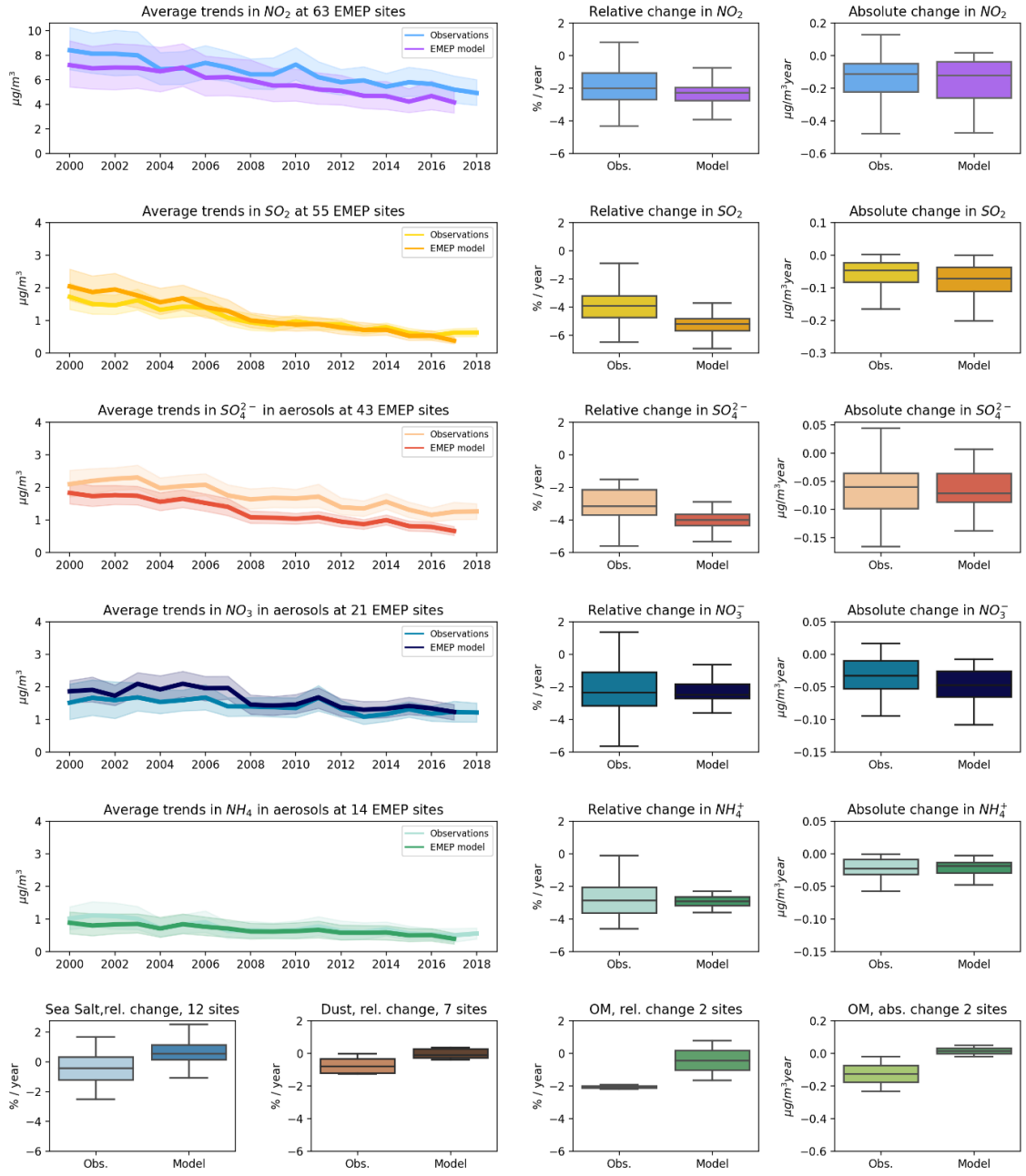

Table 2: Average trends in observations of aerosol species and precursor gases at EMEP sites from 2000-2018 compared with EMEP MSC-W model results at the same sites for 2000-2017. SIA, dust and sea salt are in PM_{10} or in aerosol with no cut off, while organic mass (OM) are in $PM_{2.5}$.

		Average absolute trend (µg/m³ y)				Average rel, trend (% /y)				No. of sites with Sign. trends	
	No. of	Observations		Model		Observations		Model			
Species	sites	Avg.	std	avg	std	avg	std	avg	std	Obs.	Model
PM_{10}	30	-0.299	0.181	-0.285	0.102	-1.69	0.86	-2.00	0.45	23	28
PM_{25}	23	-0.287	0.235	-0.272	0.108	-2.26	1.06	-2.61	0.47	18	20
SO_4	43	-0.067	0.047	-0.069	0.042	-2.90	1.56	-4.00	1.14	42	42
NH_4	14	-0.024	0.018	-0.024	0.018	-2.84	1.21	-2.93	0.42	10	14
NO_3	21	-0.034	0.042	-0.046	0.027	-1.90	2.90	-2.32	0.78	17	19
OM	2	-0.126	0.150	0.014	0.050	-2.07	0.20	-0.44	1.73	2	1
Dust	7	-0.006	0.004	0.000	0.004	-1.18	1.45	-0.22	1.79	1	1
Sea Salt	13	-0.002	0.058	0.014	0.020	-0.33	1.49	0.57	0.99	4	0
SO_2	55	-0.062	0.059	-0.096	0.097	-4.01	1.56	-5.32	1.36	46	54
NO_2	62	-0.146	0.155	-0.193	0.244	-1.51	3.04	-2.34	0.89	47	58

4.4 Trends in PM_{10} and $PM_{2.5}$ and source contributions

Trends in the PM_{10} and $PM_{2.5}$ concentrations at the respective 30 and 23 EMEP sites with long term observations are presented in Figure 24, compared with EMEP model results at the same sites, and along with the trend in modelled contribution of SIA components and changes in the contribution from the different activity sectors at the same sites. The absolute reductions in aerosol mass are similar in the two size fraction and comparable between model and observations (ca 0.28 µg mg^{-3} y^{-1}), while the percentage annual reductions are higher in $PM_{2.5}$ than in PM_{10}, and higher in the model compared to what is observed (Table 2). The largest contributions to the PM_{10} reductions appear to be due to the decrease in sulphate concentrations. For the observed sulphate trends (Table 2), sulphate seems to explain 22% of the observed trends in PM_{10}. While the model results, when only looking at consistent trend at the same sites, show that sulphate on average explains 29% of the PM_{10} trend (Figure 24), and slightly more important for the $PM_{2.5}$ trend (33%).

The observed trends in organic mass (OM) at the two sites in $PM_{2.5}$ (Table 2) indicate that the reductions in organics may be just as important as sulphate, but with only two sites representing two extremes (low and high concentration areas) and large uncertainties in the trend estimates makes this difficult to assess. The model does not capture similar trends for organic mass at the high concentration site Ispra. The modelled trend of OM at all the PM sites (Figure 25) show somewhat larger reductions (ca -0.7 µg mg^{-3} y^{-1}) compared to the average for the two sites with OM observations (Table 2).

For the observations, nitrate and ammonium seems to explain similar contribution to the PM_{10} trend, around 10% each (Table 2), while the model estimate that nitrate is more important for the reduction in PM_{10} (25%), which again is more important than for the decrease in $PM_{2.5}$ (14%). The uncertainties in both observations due to loss of NH_4NO_3 on the aerosol filters, and in the model assessment of gas/aerosol distribution as well as the split between coarse and fine aerosol fractions may explain some of the reasons for these differences.

The changes in the influence from different activity source sectors are quite similar for the two size fractions (Figure 24). The relative contribution of agriculture and industry to the total PM_{10} mass has been reduced by around 30% for both sector, industry being somewhat more important for the changes in the $PM_{2.5}$ fraction (37% on average). Thus, a similar evolution is found for agriculture and industry, although they are associated to PM precursors with very different trends such as NH_3 versus

SOx or NOx for instance. A similar trend in the relative contribution is found for both sector because they remain strongly connected through the formation of secondary inorganic aerosols (esp. ammonium nitrate and ammonium sulphate). Thus, it is important to emphasise that the emission trends are not the same as trends in sector contribution due to this nonlinear relationship, the contribution from i.e. agriculture will depend on the availability of HNO_3 and SO_2 from other sectors. The relative contribution of traffic has been reduced by around 15-20% while the heating sector has had little impact according to these modelled results.

There has only been minor changes in the contributions from natural sources like sea salt and dust, seen both by observations (Table 2) and model results (Figure 25).

The steep decline in precursors around 2007-2008, especially in SO_2 as discussed in chapter 4.2 are also reflected in the PM trends. In the trends by activity sectors there is a clear decline also for this period, but most pronounced for the industrial sector.

Country specific modelled trends in PM_{10} and $PM_{2.5}$ and changes in the contribution from the different activity sectors are given in Table 3. There is some variability in the country specific trends as also reflected in the site-specific trends shown in the boxplots in Figure 25.

Figure 25: Trend in PM_{10} and $PM_{2.5}$ at EMEP sites compared with EMEP MSC-W model results at the same sites for 2000-2017. Modelled trends of inorganic components and the activity sector contribution at the same sites. Box whisker plots showing how much the different species and sector contribute to the overall PM_{10} and $PM_{2.5}$ trends.

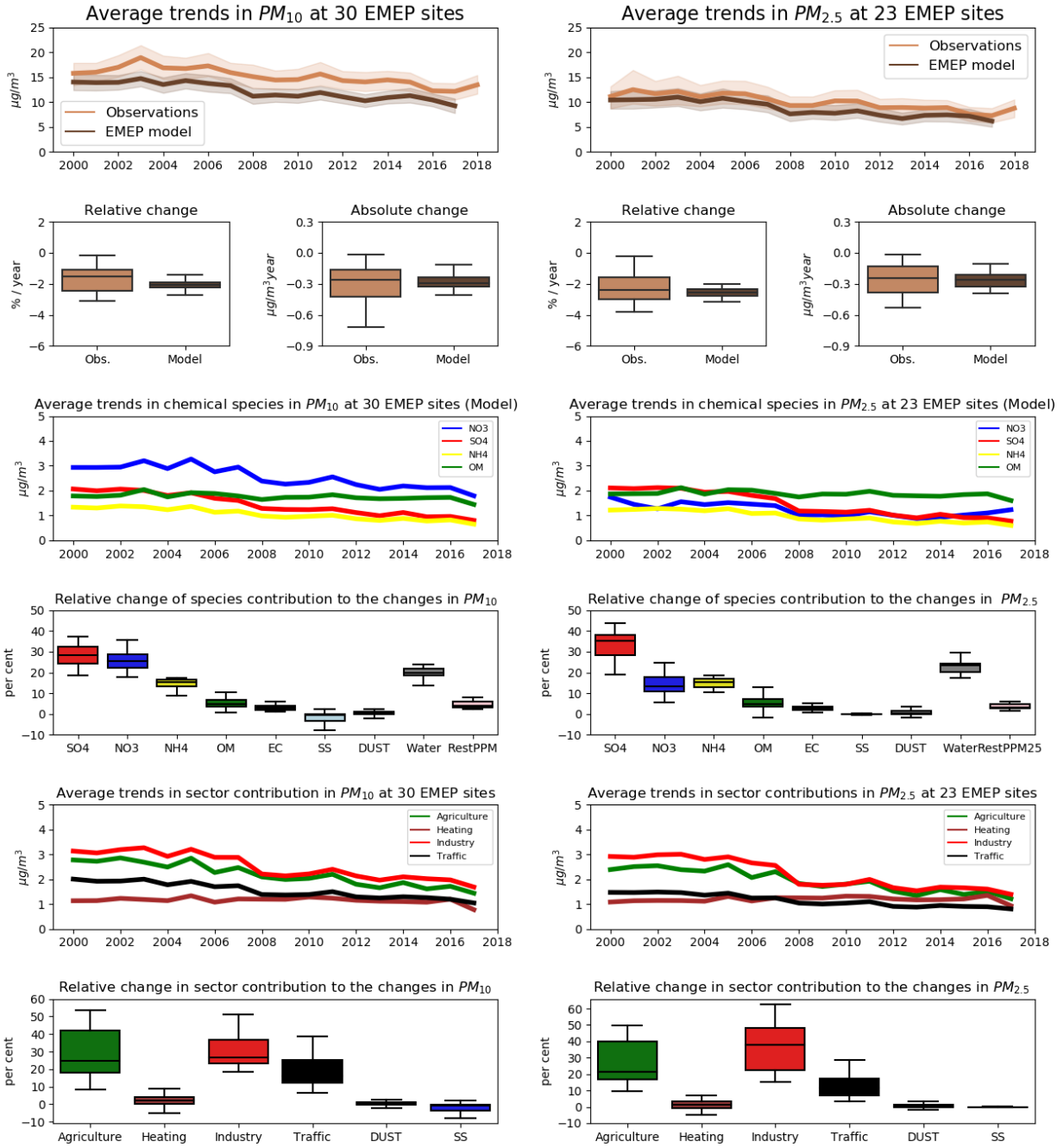

Table 3: Average modelled national trends of PM_{10} and $PM_{2.5}$ for the period 2000-2017, and trends in the contribution from the different activity sectors to PM_{10}. The trends are calculated based on the location of all EMEP sites in each country. *Only significant trends are shown. No significant trends in the contribution from sea salt and dust, thus these sectors are not included.*

Country	trend	Nr sites	PM_{10}	$PM_{2.5}$	Agriculture	Heating	Industry	Traffic
Austria	µg m^{-3} y^{-1}	20	-0.306	-0.272	-0.094	-0.014	-0.084	-0.067
	% yr^{-1}		-2.3	-2.4	-2.9	-0.8	-2.5	-2.8
Belgium	µg m^{-3} y^{-1}	7	-0.550	-0.535	-0.187	-0.028	-0.137	-0.109
	% yr^{-1}		-2.5	-2.9	-3.2	-1.3	-2.7	-3.0
Bulgaria	µg m^{-3} y^{-1}	2	-0.307	-0.249	-	-	-0.148	-0.015
	% yr^{-1}		-2.6	-2.7	-	-	-3.1	-2.7
Croatia	µg m^{-3} y^{-1}	2	-0.582	-0.506	-0.062	-0.179	-0.154	-0.054
	% yr^{-1}		-2.5	-2.8	-2.4	-3.1	-3.0	-2.6
Cyprus	µg m^{-3} y^{-1}	1	-	-0.116	-0.019	-	-	-0.034
	% yr^{-1}		-	-0.8	-2.1	-	-	-3.3
Czech Republic	µg m^{-3} y^{-1}	5	-0.302	-0.276	-0.111	-	-0.104	-0.072
	% yr^{-1}		-2.0	-2.0	-2.6	-	-2.4	-3.2
Denmark	µg m^{-3} y^{-1}	12	-0.266	-0.263	-0.100	-	-0.067	-0.043
	% yr^{-1}		-1.7	-2.6	-3.0	-	-2.7	-2.9
Estonia	µg m^{-3} y^{-1}	2	-0.134	-0.125	-	-0.006	-0.044	-0.007
	% yr^{-1}		-1.9	-2.3	-	-1.4	-2.7	-1.8
Finland	µg m^{-3} y^{-1}	13	-0.096	-0.084	-	-	-0.037	-0.006
	% yr^{-1}		-2.1	-2.3	-	-	-3.1	-2.2
France	µg m^{-3} y^{-1}	22	-0.357	-0.291	-0.088	-0.031	-0.092	-0.052
	% yr^{-1}		-2.3	-2.8	-3.2	-2.3	-3.3	-2.7
Germany	µg m^{-3} y^{-1}	1	-0.301	-0.279	-0.102	-0.011	-0.070	-0.075
	% yr^{-1}		-2.0	-2.3	-2.4	-0.8	-1.8	-2.9
Greece	µg m^{-3} y^{-1}	3	-0.433	-0.420	-0.025	-	-0.282	-0.035
	% yr^{-1}		-2.0	-2.6	-2.0	-	-3.4	-3.1
Hungary	µg m^{-3} y^{-1}	2	-0.369	-0.337	-0.117	-	-0.173	-0.053
	% yr^{-1}		-2.1	-2.1	-2.9	-	-2.9	-2.3
Iceland	µg m^{-3} y^{-1}	3	-	-	-	-	0.033	-0.002
	% yr^{-1}		-	-	-	-	4.2	-2.6
Ireland	µg m^{-3} y^{-1}	10	-0.158	-0.141	-0.050	-0.011	-0.053	-0.015
	% yr^{-1}		-1.4	-2.6	-3.0	-1.7	-3.6	-2.3
Italy	µg m^{-3} y^{-1}	8	-0.484	-0.418	-0.070	0.068	-0.169	-0.113

Country	trend	Nr sites	PM_{10}	$PM_{2.5}$	Agriculture	Heating	Industry	Traffic
	% yr^{-1}		-2.1	-2.4	-2.8	3.0	-4.1	-3.5
Latvia	µg m^{-3} y^{-1}	2	-0.150	-0.135	-0.023	-0.012	-0.043	-0.007
	% yr^{-1}		-1.8	-2.0	-1.5	-1.3	-2.0	-1.4
Lithuania	µg m^{-3} y^{-1}	2	-0.156	-0.154	-0.029	-	-0.057	-0.008
	% yr^{-1}		-1.7	-2.0	-1.4	-	-2.4	-1.2
Malta	µg m^{-3} y^{-1}	1	-0.614	-0.625	-0.067	-	-0.175	-0.053
	% yr^{-1}		-1.8	-2.6	-3.1	-	-3.9	-1.4
Netherlands	µg m^{-3} y^{-1}	7	-0.576	-0.524	-0.134	-	-0.139	-0.122
	% yr^{-1}		-2.4	-2.7	-2.5	-	-2.6	-3.1
Norway	µg m^{-3} y^{-1}	30	-0.083	-0.082	-0.013	-0.011	-0.025	-0.007
	% yr^{-1}		-1.7	-2.5	-3.1	-2.3	-3.2	-3.0
Poland	µg m^{-3} y^{-1}	5	-0.240	-0.221	-0.063	-	-0.096	-0.021
	% yr^{-1}		-1.9	-2.1	-1.9	-	-2.6	-2.0
Portµgal	µg m^{-3} y^{-1}	3	-0.313	-0.267	-0.024	-	-0.207	-0.030
	% yr^{-1}		-2.1	-2.8	-2.4	-	-5.2	-3.1
Romania	µg m^{-3} y^{-1}	2	-0.089	-0.092	0.010	-0.002	-0.055	0.006
	% yr^{-1}		-1.4	-1.7	2.2	-1.1	-2.5	2.4
Slovakia	µg m^{-3} y^{-1}	5	-0.276	-0.235	-0.051	-	-0.151	-0.023
	% yr^{-1}		-1.9	-2.0	-2.0	-	-3.3	-2.2
Slovenia	µg m^{-3} y^{-1}		-0.416	-0.379	-0.117	-	-0.179	-0.048
	% yr^{-1}		-2.5	-2.6	-3.2	-	-3.7	-2.2
Spain	µg m^{-3} y^{-1}		-0.348	-0.298	-0.053	-	-0.169	-0.041
	% yr^{-1}		-2.3	-2.9	-3.3	-	-4.9	-3.3
Sweden	µg m^{-3} y^{-1}		-0.150	-0.135	-0.041	-	-0.039	-0.017
	% yr^{-1}		-1.9	-2.5	-2.8	-	-2.8	-2.5
Switzerland	µg m^{-3} y^{-1}		-0.284	-0.268	-0.075	-0.043	-0.064	-0.094
	% yr^{-1}		-2.0	-2.2	-2.5	-2.0	-2.3	-2.5
United Kingdom	µg m^{-3} y^{-1}		-0.287	-0.254	-0.122	0.015	-0.062	-0.028
	% yr^{-1}		-2.0	-2.7	-3.3	2.7	-2.6	-2.3

5 References

Colette, A., et al., 2015, *Air Quality Trends in AIRBASE in the context of the LRTAP Convention*, ETC/ACM Technical Paper 2015/4.

Colette, A., et al., 2016, *Air pollution trends in the EMEP region between 1990 and 2012*, EMEP/CCC-Report 1/2016, NILU, Oslo (http://www.nilu.no/projects/ccc/reports/cccr1-2016.pdf) accessed 27 May 2021.

Colette, A., et al., 2017a, *Long-term air quality trends in Europe, Fine Particulate Matter ($PM_{2.5}$) Health Impacts*, ETC/ACM Technical Paper, 2017/4, Bilthoven, (https://www.eionet.europa.eu/etcs/etc-atni/products/etc-atni-reports/etcacm_tp_2017_4_aqtrendshia) accessed 27 May 2021.

Colette, A., et al., 2017b, *Long term air quality trends in Europe: Contribution of meteorological variability, natural factors and emissions*, ETC/ACM Technical Paper 2016/7, Bilthoven (https://www.eionet.europa.eu/etcs/etc-atni/products/etc-atni-reports/etcacm_tp_2016_7_aqtrendseurope) accessed 27 May 2021.

Colette, A., et al., 2018, *Long-term evolution of the impacts of ozone air pollution on agricultural yields in Europe*, ETC/ACM Technical Paper 2018/15, Bilthoven.

Colette, A., and Rouïl, L., 2020, *Air Quality Trends in Europe: 2000-2017, Assessment for surface SO_2, NO_2, Ozone, PM_{10} and $PM_{2.5}$*, ETC/ATNI Report 16/2019 (https://www.eionet.europa.eu/etcs/etc-atni/products/etc-atni-reports/etc-atni-report-16-2019-air-quality-trends-in-europe-2000-2017-assessment-for-surface-so2-no2-ozone-pm10-and-pm2-5-1) accessed 27 May 2021.

EMEP, 2018, *EMEP trends interface in Transboundary particulate matter, photo-oxidants, acidifying and eutrophying components,* EMEP Status Report. Norwegian Meteorological Institute Oslo, Norway.

EMEP, 2019, *Status Report*, Norwegian Meteorological Institute Oslo, Norway.

Hussain, M., and Mahmud, I., 2019, *pyMannKendall: a python package for non parametric Mann Kendall family of trend tests*, Journal of Open Source Software, 4, 1556, https://doi.org/10.21105/joss.01556.

Solberg, S., et al., 2018a, *Trends in measured NO_2 and PM*, ETC/ACM Report 2018/9 (https://www.eionet.europa.eu/etcs/etc-atni/products/etc-atni-reports/eionet_rep_etcacm_2018_9_no2_pm_trends) accessed 27 May 2021.

Solberg, S., et al., 2018b, *Discounting the effect of meteorology on trends in surface ozone: Development of statistical tools*, ETC/ACM Report 2017/15 (https://www.eionet.europa.eu/etcs/etc-atni/products/etc-atni-reports/etcacm_tp_2017_15_discount_meteo_on_o3_trends) accessed 27 May 2021.

Solberg, S., et al., 2020a, *Statistical modelling for long-term trends of pollutants. Use of a GAM model for the assessment of measurements of O_3, NO_2 and PM*, ETC/ATNI Report 14/2019 (https://www.eionet.europa.eu/etcs/etc-atni/products/etc-atni-reports/etc-atni-report-14-2019-statistical-modelling-for-long-term-trends-of-pollutants-use-of-a-gam-model-for-the-assessment-of-measurements-of-o3-no2-and-pm-1) accessed 27 May 2021.

Solberg, S., et al., 2020b, *Quantifying the Impact of the Covid-19 Lockdown Measures on Nitrogen Dioxide Levels Throughout Europe*, Atmosphere.

Solberg., S., et al., *Discounting the impact of meteorology to the ozone concentration trends,* ETC/ACM Technical Paper 2015/9, Bilthoven (https://www.eionet.europa.eu/etcs/etc-atni/products/etc-atni-reports/etcacm_tp_2015_9_discountmeteoo3trends) accessed 27 May 2021.

Yttri, K. E., et al., 2020, *Trends, composition, and sources of carbonaceous aerosol in the last 18 years at the Birkenes Observatory, Northern Europe*, Atmos. Chem. Phys. Discuss., 2020, 1-45, 10.5194/acp-2020-1165, 2020.

European Topic Centre on Air pollution,
transport, noise and industrial pollution
c/o NILU – Norwegian Institute for Air Research
P.O. Box 100, NO-2027 Kjeller, Norway
Tel.: +47 63 89 80 00
Email: etc.atni@nilu.no
Web : https://www.eionet.europa.eu/etcs/etc-atni

The European Topic Centre on Air pollution, transport, noise and industrial pollution (ETC/ATNI) is a consortium of European institutes under a framework partnership contract to the European Environment Agency.

European Environment Agency
European Topic Centre on Air pollution,
transport, noise and industrial pollution